

Surface heave by steam injection and subsidence by aquifer production- a 2D modeling study with Plaxis

By

Hoessein Al-Badri – 1343831

Delft University of Technology,
to be defended publicly on December 13, 2017

Supervisors:	Dr. Ir. F.C Vossepoel	TU Delft
	Prof. Dr. G. Bertotti	Tu Delft
	Dr. Ir. R.B.J. Brinkgreve	Tu Delft/ Plaxis bv Delft

2017

Abstract

Steam injection is an EOR method, which is mostly used for heavy oil production. This viable method is based on increasing the pore pressure in the reservoir and reducing the viscosity of the heavy oil. In particular cases, the increase in pore pressure and thermal expansion related to the steam injection leads to surface deformation – heave. The results show that the level of heave increases when the reservoir thickness is larger. For a 100 m thick reservoir, with a pressure increase of 5 MPa and temperature increase to 570 K, the heave is 80 mm. Increasing the reservoir thickness by a factor of two (200 m) results in an increase of heave by a factor of 1.6 (130 mm). A similar increase in heave results when we increase the pressure increment in the reservoir. In our experiments, pressure and heave are linearly related. Results depends on rock properties, most noticeably the elastic property, Young’s modulus, and thermal expansion factor. An increase in Young’s modulus leads to decrease in level of heave. An increase of thermal expansion factor leads to increase in heave.

When the water required for the steam is extracted from a shallow aquifer, producing this aquifer leads to a reduction of the level of heave that is caused by steam injection. This reduction depends on the pressure reduction in the aquifer and on its thickness. For realistic dimensions and rock properties of the aquifer, this effect appears to be insignificant. Only with very low Young’s modulus (7 GPa) and very thick aquifer, the subsidence due to water depletion can compensate the expansion caused by steam injection.

Table of Contents

Abstract	iii
List of Abbreviations.....	vi
List of Figures.....	vii
List of Tables.....	ix
1 Introduction.....	10
2 Theory.....	11
• 2.1 Injection of Steam in the Reservoir	11
2.1.1 Advantages of Steam Injection	12
2.1.2 Disadvantages of Steam Injection	13
2.1.3 Propagation and Pressure change of Steam in the Reservoir.....	14
• 2.2 Deformation	15
2.2.1 Heave at surface: Pressure and Temperature Increase	15
2.2.2 Using the aquifer for water supply	16
2.2.3 Compensate the deformation	16
• 2.3 Strain Source Models	17
2.3.1 Mogi Source Model	17
2.3.2 Geertsma Model.....	18
• 2.4 State of Steam Injection	19
2.4.1 One well model	19
2.4.2 Multiple wells	20
3 Methodology, Results and Sensitivity	21
• 3.1 1D Pressure Model	21
3.1.1 Theory.....	21
3.1.2 Creating 1D Reservoir Model	22
• 3.2 Plaxis.....	23
3.2.1 Construction of a Reservoir Model	23
3.2.2 2D model	24
3.2.3 Expectations of deformation.....	25
• 3.3 Cases.....	26
3.3.1 Comparison Analytical Solutions to Plaxis Solutions	26
3.3.2 The Influence for Reservoir Thickness	30
3.3.3 The influence of Pressure in the Reservoir and Aquifer layer	37
• 3.4 Sensitivity	38
3.4.1 Reservoir.....	38

3.4.2 Overburden	40
3.4.3 3D Plots for Reservoir and Aquifer	42
3.4.4 Extra research.....	44
4 Discussion	46
5 Conclusion	47
6 Future work	47
References.....	48
Appendix A –	49
Appendix B –.....	50
Appendix C –.....	51
Appendix D –	52
Appendix E –.....	53

List of Abbreviations

EOR	Enhanced Oil Recovery
E	Young's modulus
GPa	Giga Pascal
K	Kelvin
km	Kilometer
m	Meter
mm	Millimeter
MPa	Mega Pascal
OB	Overburden
r	Radius
R	Reservoir
RF	Recovery Factor
W	With production the aquifer
WO	Without production the aquifer
°	Poisson's ratio

List of Figures

Figure 1:A) Surface deformation caused only by steam injection. B) Surface deformation caused by steam injection and aquifer production. 10

Figure 2:The two types of steam injection A) Cycle Steam Stimulation B) Steam Assisted Gravity Drainage..... 10

Figure 3:A) The water flooding has a big fingering effect, where the water flows through the high permeable path directly to the production well. B) Due to low fingering effect, the sweep efficiency is high and piston like displacement is applicable in steam method. 13

Figure 4: Pressure-temperature relation to create steam in the reservoir 13

Figure 5: pressure change with different steam injection rate 14

Figure 6:Sketch of Mogi source model..... 18

Figure 7:Sketch of Geertsma Model..... 19

Figure 8: An injection and a production well in the reservoir 20

Figure 9: Multiple wells in the oil field "Qarn Alam" 20

Figure 10A)Pressure gradient without changing the pressure in the reservoir. B) Pressure gradient by increase pressure with 5.5 MPa in the reservoir and decrease of pressure in aquifer layer with 1.5 MPa. The abbreviations S, Aq and R are Seal, Aquifer and Reservoir, respectively. 23

Figure 11: 1) The 100 m thick reservoir. 2) The 200 m thick reservoir. The S, Aq and R are seal, Aquifer and Reservoir, respectively..... 24

Figure 12:Four different models in Plaxis:number 1,2 heterogeneous overburden, number 1,3- 1,4 and 1,5 are homogeneous overburden with limestone, sandstone and shale respectively. Here, the cluster that undergoes the pressure change is 250 m. 27

Figure 13: Resulting of heave at the surface in four different Plaxis models and Mogi model by pressure increase 28

Figure 14:Four different models in Plaxis:number 2,2 heterogeneous overburden, number 2,3-2,4 and 2,5 are homogeneous overburden with limestone, sandstone and shale respectively. Here, the cluster that undergoes the pressure change is 2500 m. 28

Figure 15: Results of surface heave in four different Plaxis models and Geertsma model..... 29

Figure 16: The 100 m thick cross section of the reservoir with different overburden aquifer thicknesses; A= 50 m, B= 100 m, C= 150 m, D= 200 m..... 31

Figure 17: Cross section of A:One injection and one production well, B: Radius of the field: Multiple Production and injection wells 31

Figure 18:Surface heave due to one injection well and one production well without producing the aquifer applied to four different aquifer thicknesses ($\alpha-1.1$) 32

Figure 19:Surface heave due to multiple injection and production wells without producing the aquifer applied to four different aquifer thicknesses ($\beta-1.1$)..... 32

Figure 20:Surface heave due to one injection well and one production well with producing the aquifer applied to four different aquifer thicknesses($\alpha-1.2$) 33

Figure 21:Surface heave due to multiple injection and production wells with producing the aquifer applied to four different aquifer thicknesses($\beta-1.2$)..... 33

Figure 22:Surface heave due to one injection well and one production well without producing the aquifer applied to four different aquifer thicknesses, for 200 m reservoir 34

Figure 23:Surface heave due to multiple injection and production wells without producing the aquifer applied to four different aquifer thicknesses, for 200 m reservoir..... 34

Figure 24:Surface heave due to multiple injection and production wells with producing the aquifer applied to four different aquifer thicknesses, for 200 m reservoir..... 35

Figure 25:Surface heave due to one injection well and one production well with producing the aquifer applied to four different aquifer thicknesses, for 200 m reservoir..... 35

Figure 26:Difference in subsidence for four realizations for 100 m and 200 m reservoir..... 36

Figure 27:Difference in subsidence for four realizations for 100 m and 200 m reservoir 36

Figure 28:Pressure change in the reservoir, without producing the aquifer..... 37

Figure 29:Pressure change in the reservoir, with producing the aquifer 37

Figure 30:Different pressure decrease in the aquifer layer..... 38

Figure 31: Varying the Young's modulus in the reservoir. The solid lines: without producing the aquifer, the dashed lines: without producing the aquifer..... 39

<i>Figure 32: Varying Poisson ratio in the reservoir. Solid lines: without producing aquifer, dashed lines: with producing the aquifer.</i>	39
<i>Figure 33: Varying Young's and Poisson's in the shale layers (seals).</i>	41
<i>Figure 34: Varying Young's and Poisson's in limestone (aquifer).</i>	41
<i>Figure 35: 3D plot of maximum heave by varying Young's modulus, reservoir thickness and pressure increase. A) Without Producing the aquifer. B) With producing the aquifer.</i>	42
<i>Figure 36: 3D plot by varying Young's modulus, thickness and pressure reduction in the aquifer.</i>	43

List of Tables

<i>Table 1: Plaxis models, Four realizations and Analytical Matlab solution.....</i>	<i>26</i>
<i>Table 2: Thickness scenarios.....</i>	<i>30</i>
<i>Table 3: Maximum heave for different aquifer thickness for single/multiple cluster model.....</i>	<i>34</i>
<i>Table 4: Maximum heave for different aquifer thickness for single/multiple cluster model.....</i>	<i>35</i>
<i>Table 5: Change in reservoir and aquifer pressure in MPa</i>	<i>37</i>
<i>Table 6: Varying Young's modulus and Poisson's ratio in the reservoir</i>	<i>39</i>
<i>Table 7: Maximum deformation (mm) by varying Young's modulus and Poisson's ratio for WO.....</i>	<i>40</i>
<i>Table 8: Varying Young's modulus and Poisson's ratio for the shale (seal) and limestone (aquifer)</i>	<i>40</i>
<i>Table 9: Maximum deformation (mm) for the aquifer</i>	<i>42</i>
<i>Table 10: Thermal expansion.....</i>	<i>44</i>
<i>Table 11: Maximal pressure increase to before creating fractures.....</i>	<i>45</i>

1 Introduction

In hydrocarbon extraction, optimizing the production is one of the key points to have a profitable project. This leads to higher recovery factor. Some fields produce by primary recovery, i.e., without injecting any agent into the reservoir Groningen gas field is an example. The pressure drop associated with production may create compaction in the reservoir and create subsidence at the surface. For another field the recovery factor increases by injecting an agent to improve the production. This is known as enhanced oil recovery (EOR). Steam injection in the reservoir is an example of an EOR method to increase the recovery factor. Inspired by a realistic case in the Middle East, Qarn Alam Field located in Oman; we simulate how steam injection in the reservoir results in surface deformation in the presence of a water-bearing layer, an aquifer, in the overburden. The overburden consists of different stratigraphic layers and is not a homogeneous overburden. This MSc thesis will investigate the next issues: How does the steam injection influence the surface deformation when the overburden layers are heterogeneous? In the case of depletion of an overlaying aquifer for steam production, how does this influence the surface deformation? And how is the depletion related to the aquifer properties? Thus, is it possible to cancel the surface deformation caused by steam injection in the reservoir by producing the aquifer? These questions will be addressed with a number of numerical simulation experiments, starting with comparison of two analytical models. All the simulation experiments are based on 2D models of a cylinder-shaped reservoir. One of the reasons why it is important to understand surface deformation is the potential damage it may cause to infrastructure and facilities at the surface. This MSc thesis may help to understand the causes of this damage and help prevent it. A better understanding of surface movement may eventually also lead to understanding of other unwanted effects such as faults reactivation and associated earthquakes as occurred in Groningen as a result of gas production.

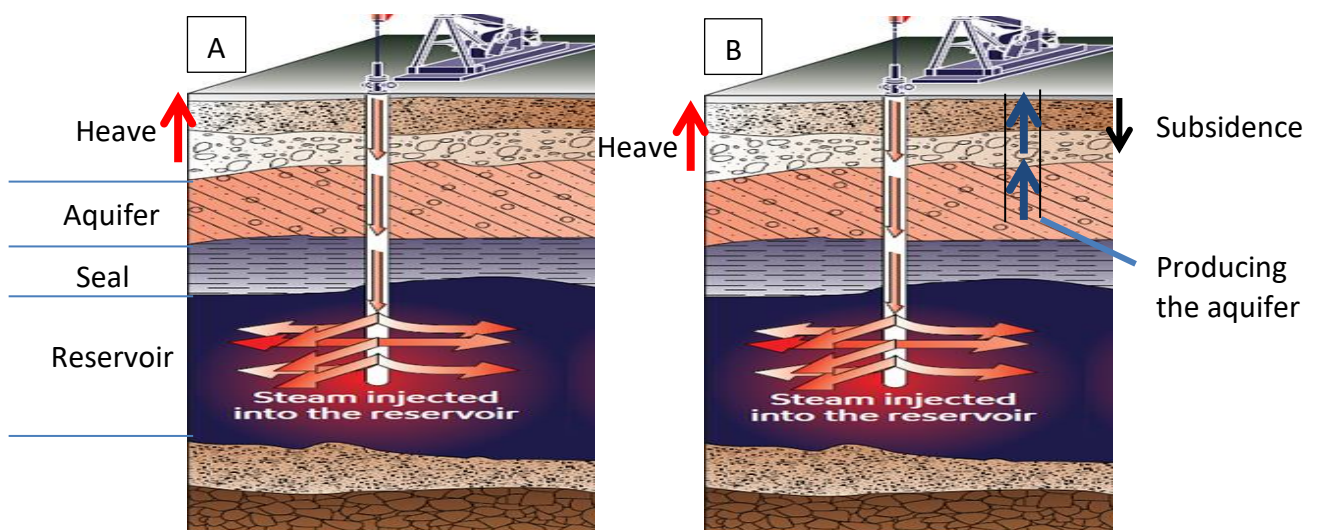


Figure 1:A) Surface deformation caused only by steam injection. B) Surface deformation caused by steam injection and aquifer production.

2 Theory

This chapter covers three different aspects of surface deformation due to steam injection: (1) the physics of steam injection and reservoir properties, (2) the effect of steam injection in the reservoir and aquifer production in the overburden of the reservoir and (3) the two analytical source models. (1) Section 2.1 describes the physics of steam injection in the reservoir, the propagation of the steam and pressure change in the reservoir. The described case and assumptions in this section forms the basis for the numerical model in Plaxis. (2) In section 2.2 I will describe briefly the effect of steam injection for the deformation at the surface. To create steam, there is water needed and this can be extracted from the aquifer in the overburden. (3) The last part describes the deformation with the aid of two analytical models, the Mogi model [3] and the Geertsma model [1]. Given the assumptions on the source of expansion, the geomechanical models of the steam injection process can approach the deformation at the surface. The application of these two models (Mogi and Geertsma) will only remain in case of pressure change.

2.1 Injection of Steam in the Reservoir

Hydrocarbon extraction knows different challenges during the production as expressed in the recovery factor (RF), which reflects the effectiveness of the hydrocarbon recovery. One of the known examples of a low recovery factor is the Qarn Alam field in Oman. The RF was expected between 3-5 percent. There are two reasons for this low RF: (1) the high oil viscosity and (2) very low matrix permeability [3]. In other fields low RFs occur as a result of rapid decrease of initial pressure [16]. Hence the case of a low RF could vary per field. To increase the RF, different methods could possibly be applied in the field. These methods are collectively named as Enhanced Oil Recovery (EOR) or tertiary recovery. It depends on the field and the hydrocarbon composition which method will be applied in the reservoir. The EOR can be categorized in three main divisions: gas, steam and chemical EOR. These three EOR categories are each subdivided in different methods. In this report we focus on the Steam injection. There are different methods to use steam in the reservoir. Cycle Steam Stimulation (CSS), Steam Assisted Gravity Drainage (SAGD) and a standard steam flooding with vertical injection and production wells are three examples how steam is used to inject in the reservoir. CSS is a method whereby a large amount of steam is injected in the reservoir and after a period of time the well is closed (soak). By closing the producing well the reservoir will be heated up and pressure will be increased. After a period of time the well will be opened and the production will restart. This method will repeat between three and seven times and is typically applied at the end of production lifetime, see figure 2-A. SAGD is a method that based on gravity difference between steam and oil. In this method, steam is injected through a horizontal well. The producer is also placed horizontal but at a deeper location than the injector, typically at the bottom of the reservoir. The steam will rise up above the injector and forms steam body. This steam body heats up the oil and pushes the oil to the producer, see figure 2-B.

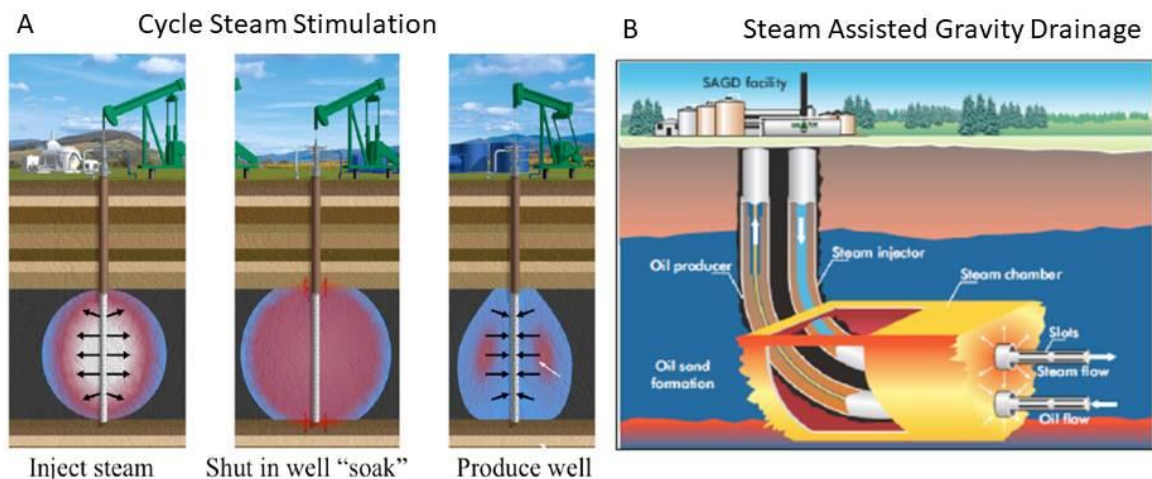


Figure 2: The two types of steam injection A) Cycle Steam Stimulation B) Steam Assisted Gravity Drainage

In this report another steam injection method is considered. It is assumed that the steam injection is injected through vertical wells. The steam will propagate in a cylindrical shape around the production wells, see figure 1. The production wells are also located vertically. In general, the steam injection is used when the viscosity of hydrocarbon is very high or for tar sands. Hydrocarbon with a high viscosity is called heavy oil. Tar sand is combination of sand, clay and water with also heavy viscous oil. In the example of Qarn Alam, the steam injection increases the RF from 3 percent to 30 percent [3]. In order to understand EOR through steam injection it is important to understand the principles and the physical propagation of the steam injection in the reservoir. The advantages and disadvantages of this EOR method will be explained in the following section.

2.1.1 Advantages of Steam Injection

Steam injection is based on injecting a heat agent in the reservoir, to decrease the viscosity of the hydrocarbon and to increase the pressure. The decrease of viscosity leads to an increase of the mobility of the oil. In general, this EOR method is used for heavy oil or tar sands. This is because the heavy oil consists of heavy molecular composition. With increasing the temperature due to steam injection in the reservoir, the high viscosity of the heavy oil decreases [16]. Even when the heavy oil is trapped in tight pore space, with the aid of this method, the trapped heavy oil is more moveable [3]. Steam injection creates higher pressure in the pores to push the hydrocarbons to the direction of the production well [16]. The third advantage of injecting steam in the reservoir is the sweep efficiency. Fingering effect is a phenomenon that occurs by injecting an agency in the reservoir and is often observed in case of water injection. This agency flows in the higher permeable path and leaving the low permeable areas. In the case of EOR with steam injection however, the fingering effect is very small. When the fingering effect is low, the propagation of this agency will be equal over the entire area. This leads to have a very low (hydrocarbon) oil saturation in the areas behind the steam front. In some areas in the produced reservoir, the remaining oil saturation is only two percent [16]. This can be seen as a piston like, equal propagation over the entire area, displacement. Figure 3 shows the difference between using water flooding, where fingering effect have lower sweep efficiency than steam injection with higher sweep efficiency.

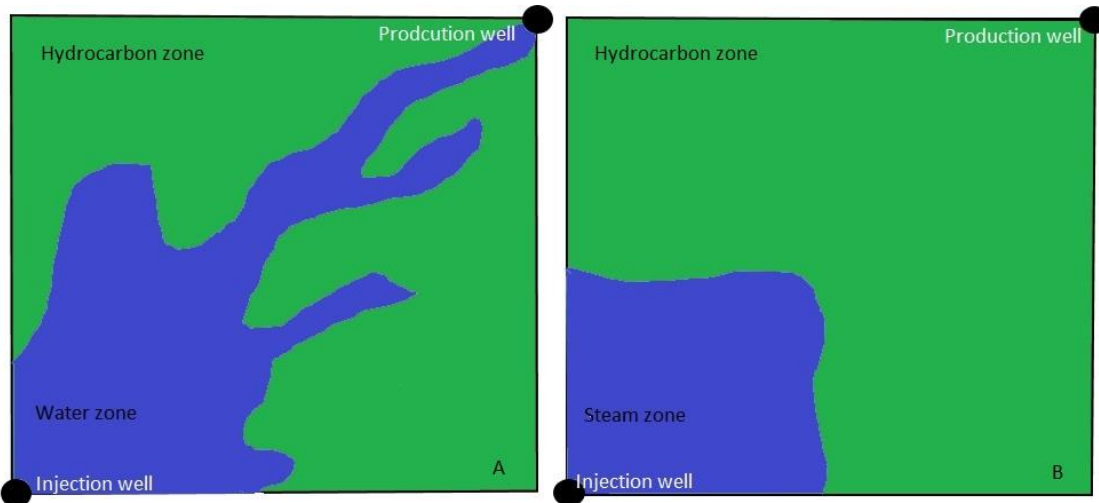


Figure 3:A) The water flooding has a big fingering effect, where the water flows through the high permeable path directly to the production well. B) Due to low fingering effect, the sweep efficiency is high and piston like displacement is applicable in steam method.

2.1.2 Disadvantages of Steam Injection

The disadvantages of using steam injection are efficiency factors. Firstly, the creation of steam makes the method expensive. Furthermore, the heat losses to the surrounding layers, the under and over layers, create heat expansion (this will be explained in chapter 2.2.1).

The third factor is related to the reservoir pressure and the temperature to create steam. When the pore pressure is high, the temperature to create steam will be also high. The next figure shows the relation between pressure and the needed temperature to create steam.

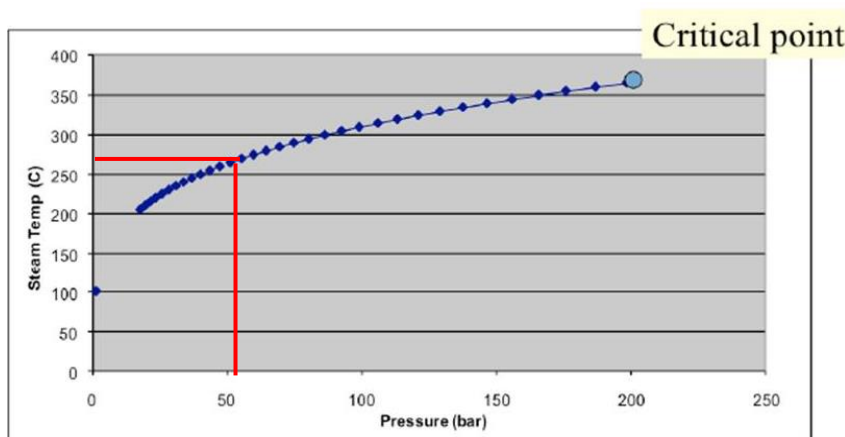


Figure 4: Pressure-temperature relation to create steam in the reservoir

The difference in density between steam and pore content in the reservoir creates difference in gravity. Since the density of steam is very low compares with oil or hot water, this will lead the steam to have a tendency to override the oil (and hot water). The length at which the separation occurs is called the *critical length*. The critical length depends on different parameters. For this reason the distance between the injection well and production well is small. In Qarn Alam, the distance between injector and producer is about 350 m [3]. In a typical water flooding case, the distance between the two is about 500 m [16].

2.1.3 Propagation and Pressure change of Steam in the Reservoir

In this study, two assumptions have been made for steam development in the reservoir. It has been assumed that the steam in the reservoir will propagate radially from the injection well and the steam zone will be developed as a piston. The radius propagation of steam is related to the injection rate. The radius of steam body is also depends on time. The steam body in the cross section can be approximated with a disk and estimated as a function of time using the following equations [11]:

$$r = 6 * t^{0.5} \quad (2.1)$$

$$r = 4.2 * t^{0.5} \quad (2.2)$$

Where r [m] is the radius of the steam body in the reservoir and the t [day] is the time or duration of the steam injection in the reservoir. The equations 2.1 and 2.2 for the radius estimation of steam body are for the injection rates 1000 and 500 ton/day [t/d], respectively. With the aid of these two equations we can also estimate the radius of a disk shaped steam body in case of lower injection rate. The exponential factor (0.5) is in both equations the same. Only the multiplication factor is different. By using a magnification factor for the injection rate, we can obtain the following equation for an injection rate about 175 [t/d]:

$$r = 2.3 * t^{0.5} \quad (2.3)$$

The pressure increase in the reservoir caused by the steam injection depends on the injection rate and the depth of the reservoir. To measure this increase for a specific depth and injection rate, typically a well test is being carried out. The change of reservoir pressure caused by the steam injection is then derived from [7]. In this test, three different injection rates are tested, to measure the pressure increase in the casing, as shows in figure 5. In this figure is the volume of injection is given by ton per hour t/h.

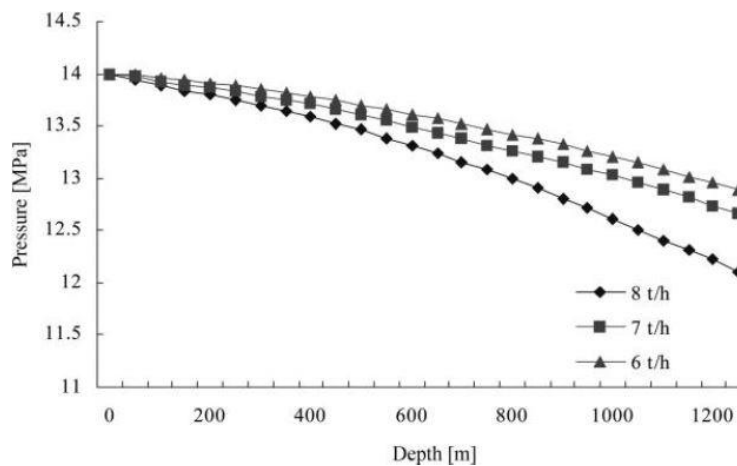


Figure 5: pressure change with different steam injection rate

As it shown in figure 5, the initial tubing head pressure for these three injection rates are the same. The change in pressure starts when the steam is moved from the top to the bottom of the well. The pressure drop in this figure indicated with 8 t/h is caused by two factors: friction and acceleration. When the flow rate increases, the pressure drop increases too [7].

In the following, the pressure increase due to the steam injection will be assumed from figure 5 and applied to 1D reservoir model in chapter 3.1.

In the following, we assume the pressure to be constant over the entire steam zone, assuming piston-like steam displacement. This implies that when the pressure changes in the reservoir, this effect will be observable in the entire reservoir. In the steady state pressure behavior, the pressure is assumed to be the same in that part of the reservoir. To illustrate the pressure change in the reservoir from the injection well to the production well, three different figures are shown in appendix B [AES150 simulation coarse]. These three figures illustrate the development of pressure for three different time frames. From this it can be concluded that any pressure can be achieved by choosing the corresponding initial pressure at the tubing head of injection well and corresponding flow rate resulting in a fixed pressure over the modeled reservoir.

2.2 Deformation

Pressure change in the reservoir causes deformation at the surface due to the expansion of the reservoir. Pressure (and temperature) increase in the reservoir causes heave [5]. On the other hand, a pressure reduction in the reservoir causes compaction, thus subsidence [1]. As mentioned before, steam injection also causes the thermal increase in the reservoir and surrounding layers. The deformation that is caused by steam injection can be followed from the pressure and temperature in the reservoir. The use of steam injection in the reservoir needs water supply. This can be produced and supplied from an aquifer, which is assumed to be at a shallower depth than the reservoir. Producing water from the aquifer layer can create subsidence, since the aquifer will compact. The subsidence due to aquifer production, resulting from the compaction of the aquifer, can compensate the heave from the steam injection at the surface.

2.2.1 Heave at surface: Pressure and Temperature Increase

The change in the subsurface by steam injection is not only due to the pressure change but also due to the thermal expansion resulting from the temperature change. The results of heave due to steam injection have been simulated and published by *Wong (2008 [2])*. These tests performed by *Wong (2008 [2])*, however, only concern the volume changes of injection and temperature change in the reservoir, without taking the secondary effects of the overburden into account. In this report the conditions in the reservoir and the overburden are included in the estimation of the surface deformation.

The effect of pressure increase in the reservoir is explained earlier. This increase can lead to a heave at the surface. To understand the dependency of pressure on the heave level, different pressure increments in the reservoir have been considered. Also, the reservoir thickness has been varied.

The effect of thermal expansion for the reservoir and surrounding layers is important in this process. The temperature needed to create steam depends on the reservoir pressure, as is shown in figure 3. Thermal expansion of the rock depends on the increase in temperature. The values for thermal expansion for the different rocks are used from literature [19]. For the thermal distribution in the surrounding layers (under and over layers) an analytical method has been used [12]. This method is applied in a 2D model to have a more realistic model and

accurate heave. The following analytical model has been used for the temperature increase [12]:

$$T_2 = T_1 - \varphi'' \frac{D}{\lambda} \quad (2.4)$$

Here, T_1 is known temperature at the reservoir edge and T_2 is the unknown temperature at the opposite reservoir edge in [K]. D is the thickness for the under and over layer, individually. The parameters φ'' [kW/m^2] and λ [$\text{kW}/\text{m}/\text{K}$] are thermal flux and thermal conductivity coefficient, respectively.

2.2.2 Using the aquifer for water supply

To create steam water is needed. There are two points important for the water supply: The costs of transporting water and the continuous of supply of water. In the example of Qarn Alam field, the water supply is from the aquifer. For this solution there costs are lower than transporting water from sea. The continuous production from the aquifer is ensured by using multiple wells. The supply of water from the aquifer is adjusted to the demand of injected steam. In the same example (Qarn Alam), the drilled wells to produce the aquifer for water supply (60 wells) are more numerous than the injection and production wells together (total of 48 wells)[4]. This indicates the huge amount of water supply for create steam. This can be achieved by a huge confined aquifer or unconfined aquifer. The compaction may cause subsidence at the surface. There are different factors that affect the subsidence at the surface, as pressure reduction, aquifer thickness and the geo mechanical properties of the rock.

2.2.3 Compensate the deformation

In this part we will sum all the factors that can affect the deformation at the surface as described in earlier chapters. As it mentioned before (chapter 2.2.1) steam injection has two effects that creates heave: pressure and temperature expansion. The thermal expansion will also affect the surrounding layers of the reservoir. The aquifer located in the overburden of the reservoir will be compacted (chapter 2.2.2). The expectation is that the pressure and thermal expansion have a bigger effect to create heave compared to the subsidence due to compaction in the aquifer layer. The level of heave will be higher when the aquifer is not produced. Thus, when the aquifer will be produced the level of heave at the surface will be lower, but the heave will be noticeable.

The main questions are: What is the level of heave caused by steam injection in the reservoir by varying the thickness, pressure increase and the elastic properties? What are the effects of varying the aquifer thickness, pressure drop and elastic properties by producing aquifer above the reservoir to compensate the heave with the subsidence? So, is it possible to cancel the heave with producing the aquifer?

The factors that affect the deformation will be varied to understand how large each factor individually effects the deformation. In this report the depth of the reservoir will not be varied and take one depth. The elasticity parameters- Young's modulus and Poisson's ratio-

can also effect the deformation. These different factors and parameters will be tested to understand the model sensitivity.

2.3 Strain Source Models

The expansion due to steam injection can be approached with the use of different analytical models. The two models considered here are the Mogi source model and the Geertsma model. They model how the pressure changes in the reservoir and relates to the surface deformation. Both models assume an ideal semi-infinite elastic rock, a so-called *elastic half-space*, which means that the overburden rock is an elastic and homogeneous rock. Therefore, any change in the reservoir will cause change at the surface.

2.3.1 Mogi Source Model

The Mogi source (1958) is defined in an elastic half space. This model is based on a point (spheroidal cavity) pressure. This model was originally created for volcanic, magma chambers. The change of pressure or volume in this cavity will lead to a deformation in the subsurface. This change in the subsurface causes uplift at the surface. The displacement is axisymmetric and directly above the source. This model assumes that the radius of the point pressure (α) is smaller in comparison to the depth (d). Figure 6 shows a sketch of the Mogi source model. The displacement at the surface for a 3D deformation is given by:

$$\begin{pmatrix} u \\ v \\ w \end{pmatrix} = \alpha^3 * \Delta P \frac{1-\nu}{G} \begin{pmatrix} \frac{x}{R^3} \\ \frac{y}{R^3} \\ \frac{d}{R^3} \end{pmatrix} \quad (2.5)$$

Whereby ΔP is the pressure change [MPa]. The ν and G are the Poisson's ratio [-] and shear modulus [MPa], respectively. The variables u , v and w are the components of the displacement vectors in the three orthogonal directions (x,y,z) at the surface locations ($x,y,0$), as indicated in the figure. The pressure has a relation with the change in volume ΔV . This is shown in the next equation:

$$\Delta P = \frac{G}{\pi * \alpha^3} * \Delta V \quad (2.6)$$

By replacing the volume change with the pressure change and using only the u and w direction (2D view) the equation will be:

$$\begin{pmatrix} u \\ 0 \\ w \end{pmatrix} = \Delta V \frac{1-\nu}{\pi} \begin{pmatrix} \frac{x}{R^3} \\ 0 \\ \frac{d}{R^3} \end{pmatrix} \quad (2.7)$$

In this equation (2.3), is shown that the volume change, depth and Poisson's ratio influence the surface displacement.

The limitation of this model is that it only takes into account the Poisson's ratio of the rock, while neglecting the other rock properties. Also, there is no explicit modeling of the reservoir

layer and the overburden. Despite the simplification of this source model still used¹ method for deformation at the surface.

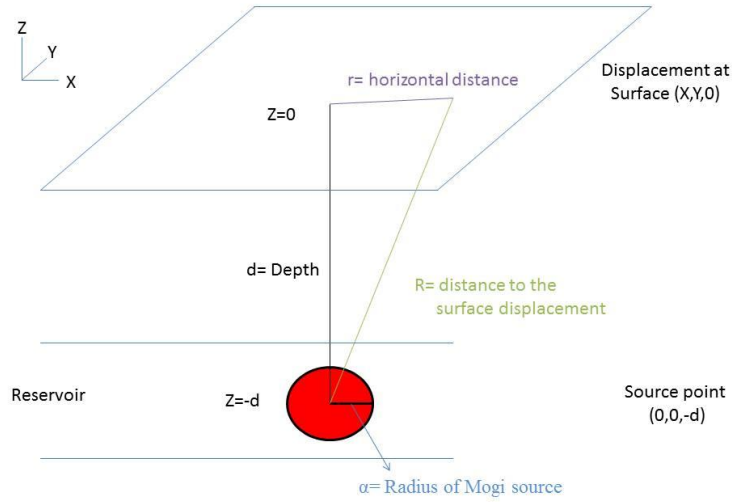


Figure 6: Sketch of Mogi source model

2.3.2 Geertsma Model

The Geertsma model (1973) is originally created for the subsidence of the surface, due to the production of hydrocarbon. This model can be considered as an extension of the Mogi source model, considering it as set of distributed strain sources that form a disc/cylindrical shape representing a compacting reservoir. As mentioned earlier, this model assumes that the entire half-space is homogeneous. In this thesis, the model is used to describe the uplift due to steam injection, which is the opposite of the original use of the model for subsidence because of production. The Geertsma model assumes an elastic and homogeneous overburden. The expansion of the reservoir results in uplift at the surface. The shape of the deformation can be expressed in the following equation:

$$u_z(r, 0) = -2Cm * \Delta P(1 - \nu) * H * R * \int_0^{\infty} e^{-Da} J_1(aR) J_0(ar) da \quad (2.8)$$

Whereby H and R are the reservoir thickness [m] and radius of the reservoir [m], respectively. u_z is the displacement at the surface [m] and ΔP is the pressure change [MPa]. ν is the Poisson's ratio and Cm is the compressibility [1/MPa].

The integration is provided as a function of the two dimensionless ratios $\rho = r/R$ and $\eta = D/R$ (here, r is the distance from the well and D is the reservoir depth). This integration is called A for the deformation in the Z direction and the deformation will be in vertical (z) and radial (r) direction. The integration table A is shown in appendix A. The shorthand notation of equation 2.8 is:

$$u_z(r, 0) = -2Cm * \Delta P(1 - \nu) * H * A(\rho, \eta) \quad (2.9)$$

¹) This model is used by two colleagues (Maarten Nieuwenhuijsen and Karin) for their master thesis (2016)

The Geertsma model takes into account the elastic properties of a rock type C_m and Poisson's ratio. The elastic property of the Young's modulus is indirectly expressed in C_m . C_m and ν are assumed to be constant over the entire half-space. Since this model is used for pressure increase and not pressure drop in the reservoir, the minus in the equation changes to a positive sign.

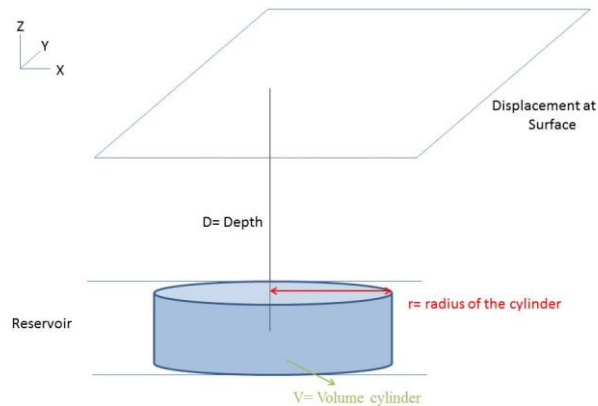


Figure 7: Sketch of Geertsma Model

This model is commonly used to determine the level of deformation (subsidence) at the surface for compacting reservoir. In a recent study² (NAM, 2016) for surface deformation for the gas field, Ameland (the Netherlands), this model is compared with numerical models that are used by NAM. The resulting deformations were close to each other.

The limitation of the Geertsma model is that the rock properties like porosity and permeability are being neglected. Also the overburden as well as the reservoir is assumed to be homogeneous.

2.4 State of Steam Injection

Since the Mogi source model and the Geertsma model are well defined, it is possible to apply these two models of the deformation in the reservoir caused by steam injection. To simplify this computation, two reservoir configurations are being considered: (1) one injection and one production well (small area) and (2) multiple injection and production wells (total reservoir). The outcome of the two analytical models will be compared with the outcome of a numerical model.

2.4.1 One well model

When considering a small area, the deformation is expected to be comparable to the deformation obtained with the Mogi source model. In this case, consider a reservoir with one injection and one production well, figure 8, where the distance between the two wells is small (250 m). The comparison of the numerical model with the Mogi source model will be carried out by applying the pressure change and disregarding the. The Mogi source model has been coded in Matlab [13] and the numerical model has been constructed using Plaxis.

²) Samenvatting van de bespreking tussen "LongTermSubsidence-II" onderzoekers en Wadden belanghebbenden. NAM, Assen. 29-9-2016

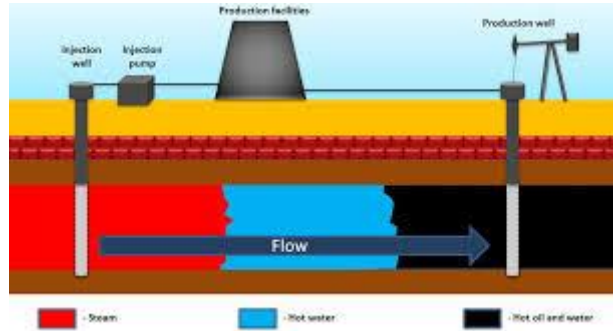


Figure 8: An injection and a production well in the reservoir

2.4.2 Multiple wells

In later stage of reservoir development, more than one well will be drilled. Rather than comparing the subsidence with the Mogi source model, this configuration will be compared with Geertsma model which assumes the reservoir as a disc/cylindrical shape. The numerical model of the reservoir in Plaxis, will have the same size and shape. In this configuration the radius will be larger (2500 m) than in the one-well case modeled with Mogi source. Again, only the pressure will be changed, neglecting the effects of a temperature change. The reason to test and use the Geertsma model is to understand the deformation over the whole reservoir. In reality the deformation will not be limited to the area around one single well. In a realistic case such as Qarn Alam, the deformation happens over total reservoir, as is shown in figure 9.

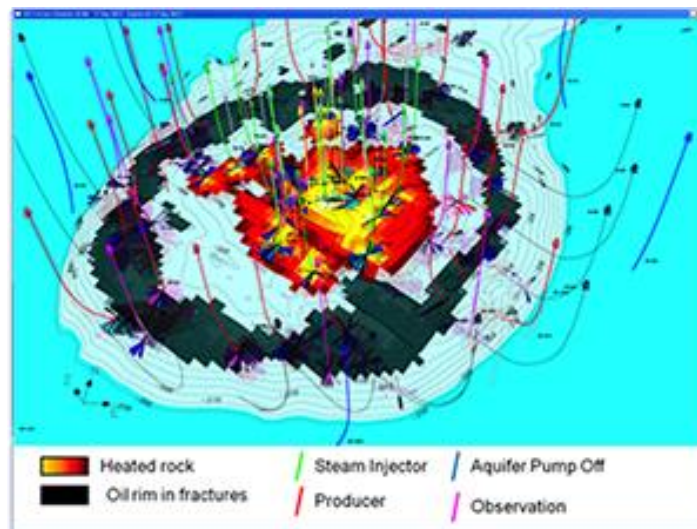


Figure 9: Multiple wells in the oil field "Qarn Alam"

3 Methodology, Results and Sensitivity

This chapter describes the various models used in this thesis. It starts with description of a 1D reservoir pressure model. With this model, I will aim to estimate (1) the initial pore pressure in the reservoir, (2) the increase of the pore pressure without creating fractures and (3) the confining pressure. These three points will be used directly and indirectly for the necessary boundary conditions for the numerical reservoir model. This numerical reservoir model will be created by using the Plaxis modeling package. Plaxis is a numerical tool and is based on the Finite Element Method (FEM). The pore pressure from the 1D pressure model is used to observe the maximum pressure increase. Secondly, the pore pressure will be used to estimate the necessary temperature increase for creating steam, making use of figure 4. The confining pressure will be used to estimate the elasticity parameters in the numerical model.

The second part will study the difference between the two analytical models and the numerical model when increasing the pressure. In this part, I will also study the sensitivity of heave to changes in the thickness of the reservoir and aquifer and changes in pressure for both layers. For these two scenarios will provide the effect of producing the aquifer (chapter 2.2.1 and 2.2.2).

The last part will study the effect of elastic properties. This is done for the reservoir rock, the seal and the aquifer layer. I will also study the level of heave by varying the Young's modulus, the thickness in combination by varying the pressure change for the reservoir and the aquifer. This is provided in a 3D plot. The last section will study the effect of thermal expansion, maximum pressure increase before creating fractures model.

3.1 1D Pressure Model

In this chapter I will explain the theory and the used equations for the 1D pressure model. This 1D model will represent the lithostatic and hydrostatic pressure gradients. Secondly, I will apply the pressure change in the reservoir and aquifer. The obtained values of pore pressure, lithostatic/hydrostatic pressure and the allowable pressure increase in the reservoir will be applied directly and indirectly in the numerical model.

3.1.1 Theory

The pressure gradient can be split in two parts, namely the pore pressure gradient (hydrostatic pressure gradient) and lithostatic pressure gradient. The lithostatic pressure gradient is also referred as the confining pressure gradient. The equation for the lithostatic pressure gradient reads [6]:

$$P_{lith} = ((1 - \varphi) * \rho_{rock} + \varphi * \rho_{water}) * D * g \quad (3.1)$$

Here, P is the lithostatic pressure, the φ and ρ are porosity [-] and density [g/cm³], respectively. D is the depth of the reservoir and g is the acceleration due to gravity (9.8 m/s²).

The pore pressure or the hydraulic gradient is shown in next equation [9]:

$$P_{pf} = \rho_{fluid} * D * g \quad (3.2)$$

Let's assume that the upper and lower part of the reservoir contain water. In the remaining part of the reservoir, the pore content is oil. These types of hydrocarbon have a different density than water.

Hydrocarbons are trapped in different types of rocks. A reservoir rock can be sandstone, carbonate or even shale. Knowing the lithology of the reservoir is important for the proper understanding of the behavior of displacement. In general, each lithology has its own set of geo mechanical parameters and properties. In order to calculate the deformation in the reservoir, we need to know the elastic properties of the reservoir, namely the Poisson's ratio and Young's modulus. For a specific reservoir rock these properties can be tested in a laboratory on a sample of reservoir rock. Typical values for various rock types have been documented in the literature [21] (Appendix D shows the possible elastic properties). In general, the confining pressure [17] or effective pressure³ is related to the compressional wave velocity (V_p). Different laboratory tests show that the compressional wave velocity is almost constant when the (confining or effective) pressure increases. On the other hand the compressional wave velocity has a theoretical relation to the Young's modulus [18].

3.1.2 Creating 1D Reservoir Model

For this study, a 1D reservoir model is made in order to define the boundary conditions for the numerical model. The reservoir depth is 500 m below the surface. So the constructed reservoir is shallow and has no gas cap; the oil-water-contact at 600 m. Hence, the reservoir thickness is 100 m. The reservoir rock is a limestone, with rock properties taken from an analogue in the Middle East [18] [3]. The reservoir at the top is sealed by a 50 m thick shale layer. The porosity of the reservoir rock is 30 percent; the rock density is 2.6 g/cm^3 . The water and oil densities are 1.1 and 0.93 g/cm^3 , respectively.

In the overburden, an aquifer is modeled above the seal, which implies that the bottom of the aquifer is at the depth of 450 m. The influence of the aquifer on the overall compaction of the subsurface and subsidence at the surface is modeled for different values of aquifer thickness and pressure drop. The aquifer rock is limestone, like the reservoir rock. The porosity of the aquifer is 35 percent. In the base case of the 1D model, the aquifer thickness is 100 m. The 50 m thick shale layer above the aquifer is acting as a seal. The depth of this seal depends on the thickness of the aquifer layer.

In this study, the effects of porosity, permeability and capillary pressure changes will be neglected. Also the effect of potential faulting (fractures) will not be considered in this report. With the aid of equations 3.1 and 3.2 the lithostatic and hydrostatic pressures are calculated and the results are shown in figure 10-A. This figure shows an overpressure below the seal at the depth of 500 m. The seal kept the oil in the reservoir during the charge and in this way created an overpressure. The aquifer layer in the overburden and underburden, below the OWC, is assumed to be an unconfined aquifer. Thus, the hydrostatic pressure will be linearly from the surface downward. Using the relation discussed in 2.1.3, the pressure in the reservoir will be increased in stages to 4, 4.5, 5 and 5.5 MPa, respectively. This is done to see how big the pressure increase can be without creating fractures in the reservoir. At the same time the pressure in the aquifer layer is reduced in steps of 1, 1.5, 2 and 2.5 MPa

³) Gary Mavko, "Fracture Conceptual overview of rock and fluid factors that impact seismic velocity and impedance."

respectively. As a base case I assume a pressure increase of 5 MPa in the reservoir and a pressure decrease of 1.5 MPa in the aquifer layer. Figure 10-B shows the increase of 5.5 MPa in the reservoir and reduction of 1.5 MPa in the aquifer.

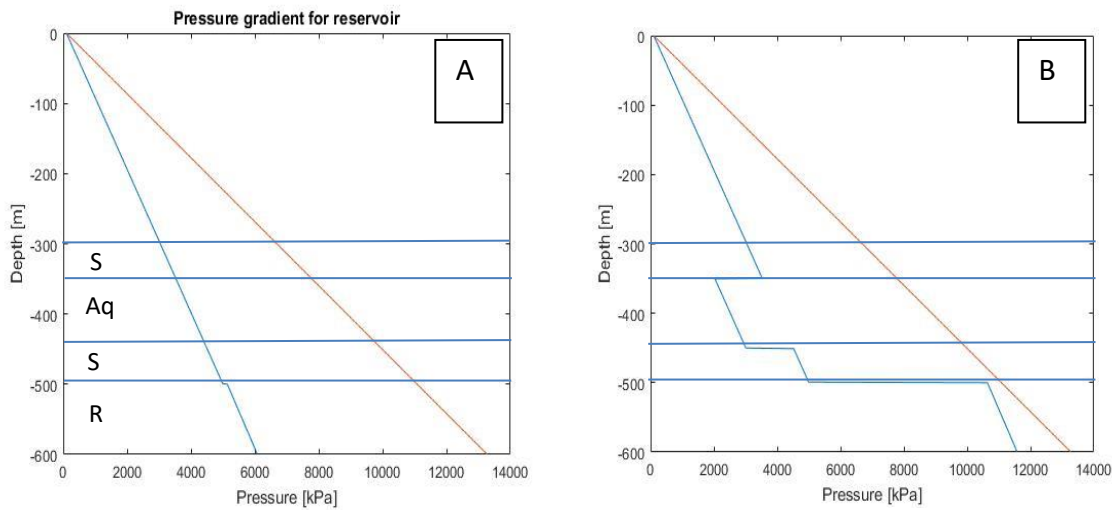


Figure 10A) Pressure gradient without changing the pressure in the reservoir. B) Pressure gradient by increase pressure with 5.5 MPa in the reservoir and decrease of pressure in aquifer layer with 1.5 MPa. The abbreviations S, Aq and R are Seal, Aquifer and Reservoir, respectively.

3.2 Plaxis

In this section we introduce the modeling tool Plaxis, which will be used for the modeling of the 2D reservoir. Plaxis is a numerical tool that based on the Finite Element Method (FEM) [16]. On the conditions that we provide the necessary input values, Plaxis creates numerical model of the subsurface. By varying these values, we can model the resulting changes in deformation and thermal expansion of the (sub) surface. I use Plaxis to investigate the level of heave due to steam injection in our reservoir model. Also, the level of subsidence due to aquifer production is investigated. Our model has different overburden layers with different geomechanical properties. In this section, the focus lies on explaining the key concepts of the Plaxis modeling tool in so far these are relevant to the research topic of this thesis. Furthermore, this section describes how these concepts are applied in our case, rather than give all the details of the geomechanical equations and concepts of Plaxis.

3.2.1 Construction of a Reservoir Model

The reservoir is modeled with a 2D axisymmetric geometry (disc shaped model), the reason being that most reservoir simulation can be considered to be disc model as a first approximation [18]; also the analytical models used in this thesis assume radius/disc models. In each layer a rectangular/polygon shape can be created, called a *cluster* (in figures 12 and 14 the arrow shows the dimension of the cluster). In this report, we have chosen for the cluster method because of the simplification of the calculations. Furthermore, we assume steady state behavior in the reservoir. After the initial transient and semi steady states the injection and production in the reservoir behaves as a steady state [16]. The interest of this research is to study the behavior of maximum changes. In each cluster, the temperature and pressure conditions can be changed. For the reservoir conditions, the pressure and temperature are changing as a result of the steam injection, as mentioned before. However, the hydrocarbon production from the reservoir causes a reduction in pressure (see appendix B for the increase and reduction of pressure in the reservoir). This pressure change as a

result from production is also taken into account in the model. Around the production wells clusters are created which cater for the decrease of pressure and the increase of temperature as a result of the produced oil that has been heated up. For these clusters, the pressure reduction is assumed to be fixed, with value of 3.5 MPa [3]. Because of heat losses to the under- and over layer (seal) the temperature increases in these two layers. By using equation 2.4 these temperature increases are applied to the surrounding layers. This is done by taking a large cluster in these two layers. For the evaluation of changes in the produced aquifer layer, we also used a different cluster. Note that for this cluster only the pressure is changed. For the base case test, 1.5 MPa decrease in pressure is used. For testing the effect of pressure change in the aquifer layer also 1, 2 and 2.5 MPa decrease in pressure is applied. For this research three different rock types are used: sandstone, shale and limestone. The rock properties such as thermal and geomechanical properties are taken from the literature. Specifically, the values from oil fields in the Middle-East are used [17] [18]. In these fields the most of hydrocarbons are trapped in limestone rock. The limestone reservoir properties are deviant from the other limestone aquifer properties, since the pore pressure and pore content influence the geomechanical properties of the limestone. As mentioned before, the shale layers are the seal. For the material models (rock behavior) of the rocks we used the Mohr Coulomb model. This model assumes linear elasticity and perfectly plasticity. For the reservoir rock a 1D model is used to read the confining pressure, which is then used to determine the compressional wave velocity [17]. With the value of compressional wave velocity the Young's modulus is defined [18]. See appendix C for the steps used to define the Young's modulus.

3.2.2 2D model

The following describes how the 2D subsurface model is defined. There are two different realizations for reservoir thickness. The first reservoir (1) will be 100 m and the second reservoir (2) will be 200 m thick. The 2D subsurface dimensions for the first reservoir are 4 Km long and 700 m deep. The dimensions of the reservoir itself are 2.5 Km by 100 m, at 500 m depth. For the reservoir (2), the subsurface dimensions are 4 m long and 800 m deep and the dimension of the reservoir are 2.5 Km by 200 m, at 500 m depth.

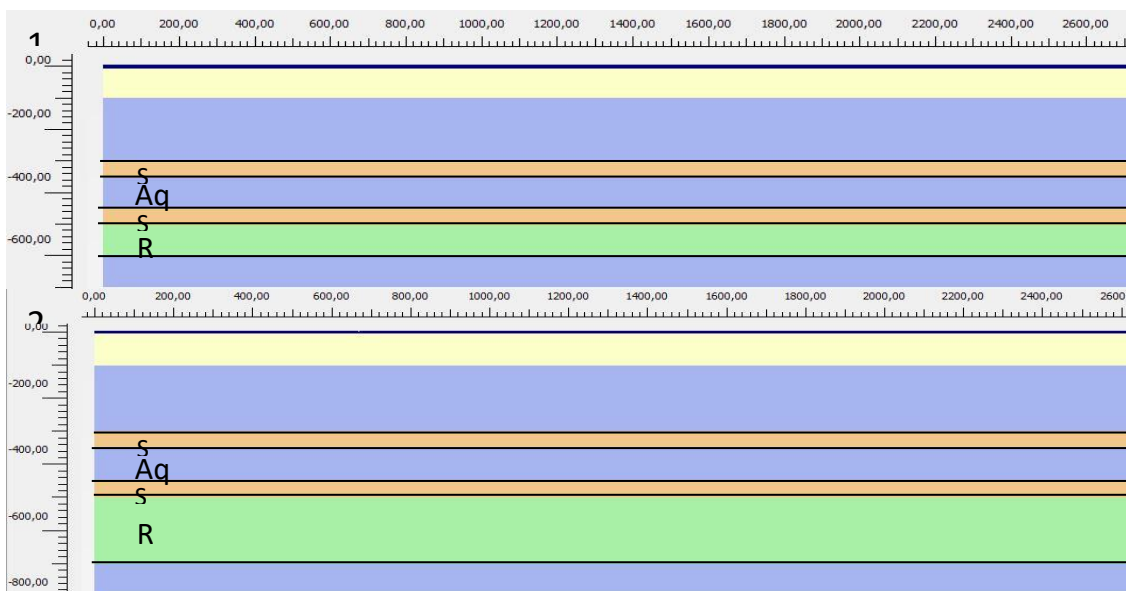


Figure 11: 1) The 100 m thick reservoir. 2) The 200 m thick reservoir. The S, Aq and R are seal, Aquifer and Reservoir, respectively

Most steam injection projects in the world are in shallow reservoirs⁴, between 100 and 600 m depth. In this report, there is no measured values to calculate the critical length for the steam zone but we assume a critical length of 200 m (see figure 17-A). This choice is made, firstly because the duration of the example oil field “Qarn Alam” is calculated to be about 30 years [10]. With equation 2.3, the radius of steam zone is calculated to be 250 m. Secondly, this is done to simplify the 2D model in Plaxis, since we include the effect of production around the production well, 50 m, and the radius of the reservoir is 2.5 Km.

The reservoir will be modeled in two steps. The first step (α) will be done by defining single injection and single production well. The single well model is chosen to clarify the effect of heave for a small area with single well. The cluster length in the reservoir for the production well is 50 m and for the injection well 200 m, see figure 17-A. For the heat losses in the surrounded layers of the reservoir and for the aquifer layer, the length is taken to be 250 m. This length is chosen because we are only interested in the deformation above the reservoir. So I neglect the deformation outside the edges of the reservoir.

The second step (β), is done by defining multiple clusters in the reservoir. The first and last clusters are 50 m, the reason being that these two clusters are at the edge of the reservoir and the production is only from one direction. The other production clusters are 100 m, since the production will be from different directions. For the injection clusters the same approach is also used. Because the injection wells are in the middle of the reservoir, the injection will be in different directions. Thus, the area for these clusters will be 200 m. For the clusters in the under- and over layers the total length of the reservoir (2.5 Km) is taken, see figure 17-B for the total reservoir.

At 500 m in the 1D model, the pore and lithostatic pressures are 5.1 MPa and 11.0 MPa, respectively. In the Plaxis model, the pore pressure is almost the same as in 1D model namely, 5.0 MPa. The lithostatic pressure is 12.5 MPa. The difference between the 1D and Plaxis model is caused by the fact that the Plaxis model takes into account the overburden.

For the temperature increase the 1D model is used to determine the reservoir pressure, resulting in a value of 5.1 MPa. With the help of figure 3 we can determine the required temperature-pressure relation needed to create steam. For 5.1 MPa a temperature increase of 265 K needed. The used temperature gradient is 0.025 m/K. The surface temperature is 293 K. At the depth of 500 m the temperature will be 305 K. Thus, the total temperature will be 570 K in the reservoir. This value is assumed to be invariable in the total steam zone. For the heat losses to the surrounded layers equation 2.4 is used. By calculating the heat losses for the surrounded layers, the thermal distribution can be computed. Appendix C shows the thermal distribution that occurs from the heat losses from the reservoir to the surrounded layers. For the three layers, reservoir and surrounded layers, the thermal expansion is assumed to be isotropic. The used values for the thermal calculations are shown in appendix D [19] [20].

3.2.3 Expectations of deformation

This part discusses which parameters/factors I expect to play large role in the deformation and which parameters/factors have a lesser effect. I divide the parameters (or factors) that I will evaluate in three different parts: (1) the Elastic properties- Young’s modulus and

⁴) Georgy Zerkalov, “Steam injection for enhanced oil recovery.” Stanford University. December 7, 2015

Poisson's ratio- (2) the specific depth and thickness of the layer and (3) the pressure-temperature increase. For point (1), the literature mostly refers to Poisson's ratio rather than Young's modulus. In the analytical and numerical solutions the Poisson's ratio is used instead of the Young's modulus [2] [4] [8] [1]. This suggests that the Poisson's ratio has a more prominent effect on the deformation than the Young's modulus. For point (2), the thickness and depth of the layer is an essential factor that determines the level of deformation. The level of deformation will be larger when the thickness of the layer is larger. For the depth this will be the opposite. The level of deformation will be larger when the layer is at shallow depth. For point (3), the expectation is that the pressure has a larger an effect on the level of deformation in comparison to the effect due to thermal expansion. This thesis will not consider the change in temperature and reservoir depth. The remaining of the parameters/factors will be tested in the next chapters.

3.3 Cases

In this section we will test and compare the various models that we have created. Firstly we will compare the two analytical solutions, provided by Mogi and Geertsma, with the numerical (Plaxis) models. The second case that we will evaluate, is a result in which we have modeled flat reservoir with flat overburden layers. The thicknesses of the reservoir and aquifer will be varied. The reservoir thickness is 100 and 200 m as mentioned before. For each reservoir, the thickness of the aquifer layer is tested by taking 50, 100, 150 and 200 m. This is done to study the behavior of the aquifer. The third case is the pressure change in the reservoir and aquifer layer. The pressure increase in the reservoir is 4, 4.5, 5 and 5.5 MPa by keeping the aquifer pressure fixed on 1.5 MPa for all the four reservoir pressures. Following that I vary the pressure reduction in the aquifer by 1, 1.5, 2 and 2.5 MPa whilst keeping the pressure in the pressure constant at a value of 5 MPa. For the two modeling the thickness of the reservoir and aquifer layer will be 100 m.

3.3.1 Comparison Analytical Solutions to Plaxis Solutions

Four realizations in Plaxis are considered to study the effect of overburden composition on the resulting subsidence. The different realizations consist of one heterogeneous and three different homogeneous overburden cases. The three homogeneous overburden cases use different types of rocks with different parameters (limestone, sandstone and shale). The results are compared to the analytical Mogi and Geertsma models. To have a like-for-like and correct comparison, the parameter values, reservoir thicknesses, geomechanical parameters and pressure changes that are used for Mogi and Geertsma are chosen to be the same as in the Plaxis cases. Table 1 shows the different tests.

Table 1: Plaxis models, Four realizations and Analytical Matlab solution

	Matlab	Heterogeneity	Homogeneity: Limestone	Homogeneity: Sandstone	Homogeneity: Shale
(1)Mogi	(1,1)	(1,2)	(1,3)	(1,4)	(1,5)
(2)Geertsma	(2,1)	(2,2)	(2,3)	(2,4)	(2,5)

The models created in Plaxis are simplified models, meant for comparison with the two analytical models (therefore only the pressure change is applied). This comparison is meant to study how close the Plaxis results in comparison with the two analytical results are. If the deformation is the same, the use of an analytical model for heave in these reservoir configurations can be justified. The analytical results, for the first stage, are also meant to have a basic understanding of the deformation for this simplified case. For the comparison to the Mogi source model, I choose a smaller reservoir (250 m radius) than for the comparison with the Geertsma model (2.5 Km radius). In total there will be eight models in Plaxis, four models to compare Mogi and the other four to compare Geertsma, see table 1.

Mogi and Plaxis results

The first study is carried out using the Mogi source model [13]. In this test, the pressure is increased by 5 MPa and Poisson's ratio of 0.2. The radius of the Mogi source and the cluster in Plaxis are 250 m. The reservoir rock is kept the same in all the realizations, only the overburden is changed. The required parameters for each rock are given in appendix D. The overburden layers consist of sandstone (yellow), limestone (blue) and shale (brown). In the homogenous overburden cases the three different rocks are modeled separately, to test how the different rock types effect the deformation at the surface. Figure 12 illustrates the four different models in Plaxis. Figure 12-1,2 shows the real dimensions of the field. Figures 12-1,3/ 1,4 and 1,5 show a small cluster and a homogeneous overburden.

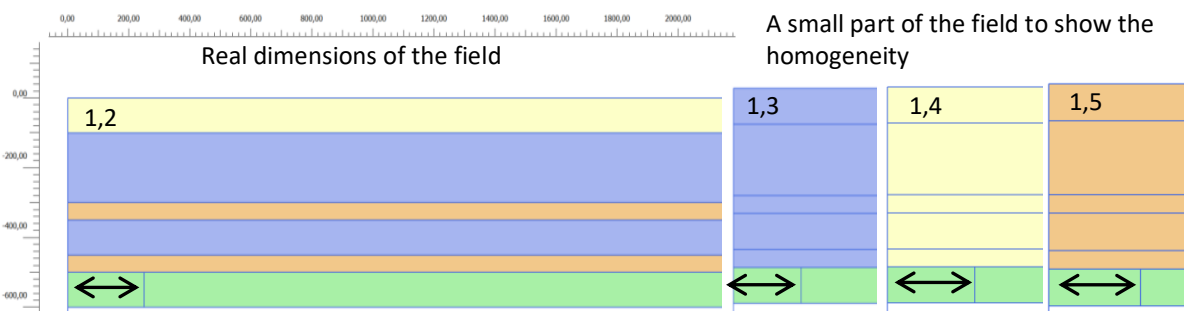


Figure 12: Four different models in Plaxis: number 1,2 heterogeneous overburden, number 1,3- 1,4 and 1,5 are homogeneous overburden with limestone, sandstone and shale respectively. Here, the cluster that undergoes the pressure change is 250 m.

In figure 12, four different models are shown. Figure 12-1,3/ 1,4 and 1,5 show the part of the field, where the reservoir is located and illustrate the homogeneous overburden, with an overburden composed of limestone, sandstone and shale, respectively. The green layer, in all the four images, is the oil reservoir rock. The reservoir undergoes a pressure change at the side closet to the symmetry axis, indicated with the black arrows in the green layer.

The four different models in Plaxis and the Mogi source model in Matlab have been run independently. The results of the Mogi and four realizations are shown in figure 13.

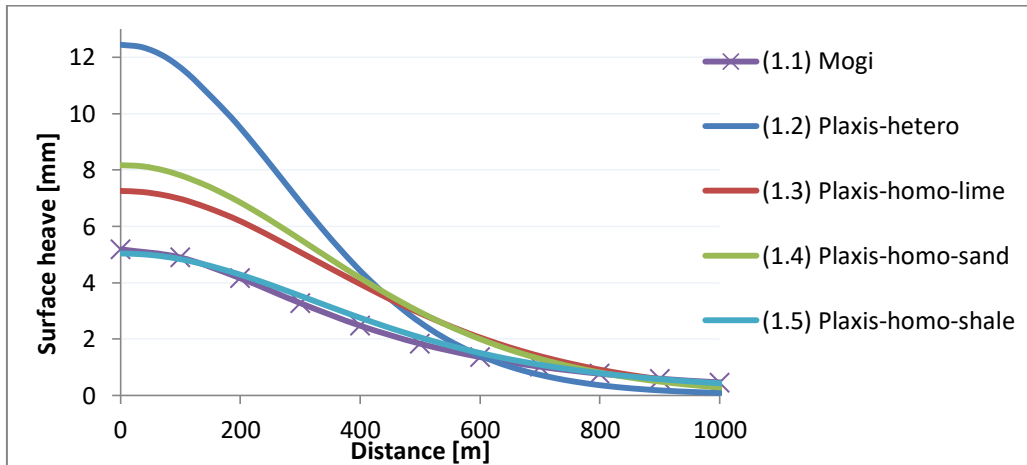


Figure 13: Resulting of heave at the surface in four different Plaxis models and Mogi model by pressure increase

The results in figure 13 are different from each other. The heterogeneous (1,2) model has a maximum deformation about 12 mm. The homogeneous shale model (1,5) corresponds to the analytical result of the Mogi model (1,1), 5.2 mm. The deformation of the homogeneous sandstone (1,4) is 7 mm and the limestone (1,3) is 8 mm. These two (1,3 and 1,4) models are close to the deformations of Mogi (1,1) and Shale (1,5). The deformation in the heterogeneous model can be explained as follows. The reason for this high deformation is caused by the 50 m thickness of shale that serves as seal above the reservoir. The geomechanical properties, namely the Young's modulus (E) and the Shear modulus (G) of shale are very low in comparison to other overburden rocks. The effect of low shear modulus causes a less resisting to undergo the deformation. So, the deformation in shale layer above the reservoir will be higher. The shale is followed by 100 m thick (blue) limestone. The limestone has a high value of Young's modulus and Shear modulus in comparison to shale. This combination creates a higher deformation at the surface. So, when the overburden is homogeneous, the results will be close to Mogi source model. The difference is when the overburden is heterogeneous.

Geertsma and Plaxis results:

The second study is aimed at comparing the results of the Geertsma model with the Plaxis models. Here, the same structure is used as in the Mogi test, namely one heterogeneous and three individual homogeneous overburden. The reservoir has a radius of 2.5 km. The pressure and Poisson's ratio are 5 MPa and 0.2, respectively. The other parameters for each rock are shown in appendix D. In figure 14, the four created models are shown.

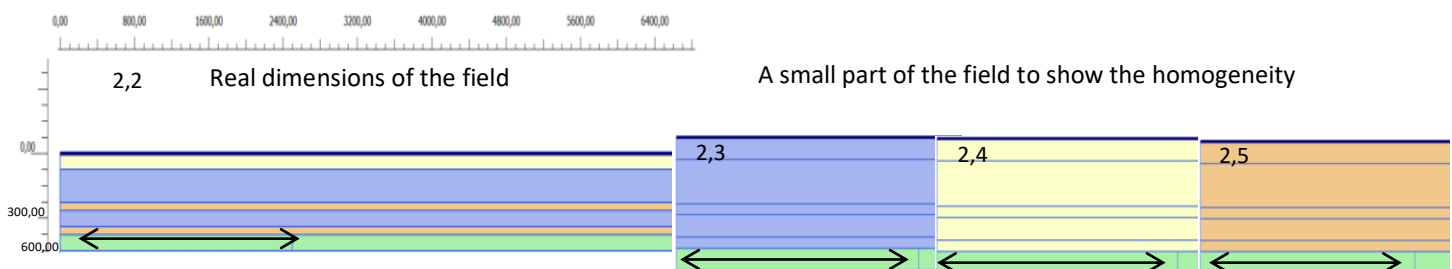


Figure 14: Four different models in Plaxis: number 2,2 heterogeneous overburden, number 2,3-2,4 and 2,5 are homogeneous overburden with limestone, sandstone and shale respectively. Here, the cluster that undergoes the pressure change is 2500 m.

Since the reservoir depth is at 500 m and the radius of the reservoir is 2.5 Km, so η ($=D/R$) will be 0.2. From the table in appendix A, the values in the column of 0.2 will be used for creating the deformation for Geertsma model in Matlab.

The results of the four Plaxis models and Geertsma model are shown in figure below.

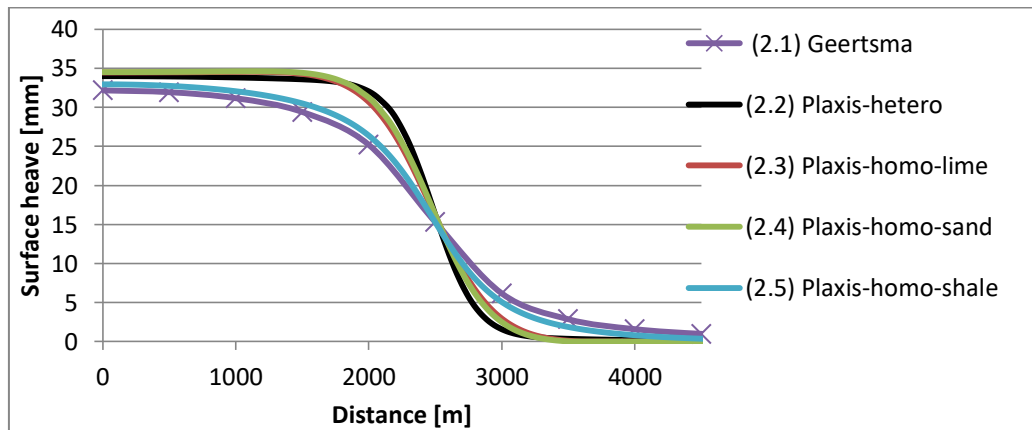


Figure 15: Results of surface heave in four different Plaxis models and Geertsma model

The results of the deformation in the second test are close to each other. Again, like the Mogi test, Geertsma and the homogeneous overburden with shale are very close to each other. Note that in this test, the deformation of the heterogeneous model is not very different from the homogeneous models. The homogeneous overburden of sandstone and limestone are almost identical in deformation.

Comparing the two tests that we have performed, we notice the following differences between the two. The first difference is the deformation level between the two tests. In the first test the deformation level is between 5 and 12 mm. In the second test, the deformation level is between 32 and 34 mm. This difference is due to the difference in area that undergoes the pressure change. The larger the area the large the deformation will be. The shear stress plays a role in the level of deformation. Since the pressure change is in a small area the effect of shear stress is high. For the first test, the domain is small, thus the shear stress at the edges ensures that the deformation will be small. In the test with larger reservoir, the area that undergoes the pressure change is larger. Given that the shear stress acts at the boundaries of the reservoir, the influence of the shear stress in the middle of the cluster there is low comparing to the boundaries. Therefore, the maximum deformation in this test is larger than in the test with the small reservoir. The second difference is the individual results in realization between tests (1) and tests (2). As it shown in figure 13 the individual differences are between 5 and 12 cm. In figure 15, the differences are between 32 and 34 cm. This means, when the pressure change occurs in a large area (2), the influence of the overburden is smaller than when the pressure change occurs in a smaller area (1). The third difference is the deformation beyond the boundary of the cluster. In tests (1), the deformation at the surface goes further than the boundary of the cluster (250 m). After 500 m the deformation is less than the half of the total deformation. The slope is obtuse between the top of the deformation and the normal ground level. On the other hand the deformation in the second tests extends much less beyond the cluster. At the boundary of the cluster at the surface, the deformation is half of the maximum deformation. There is a very sharp slope between the top of the deformation and the reference surface level.

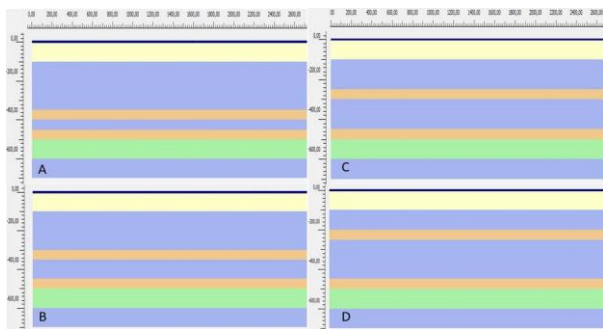


Figure 16: The 100 m thick cross section of the reservoir with different overburden aquifer thicknesses; A= 50 m, B= 100 m, C= 150 m, D= 200 m

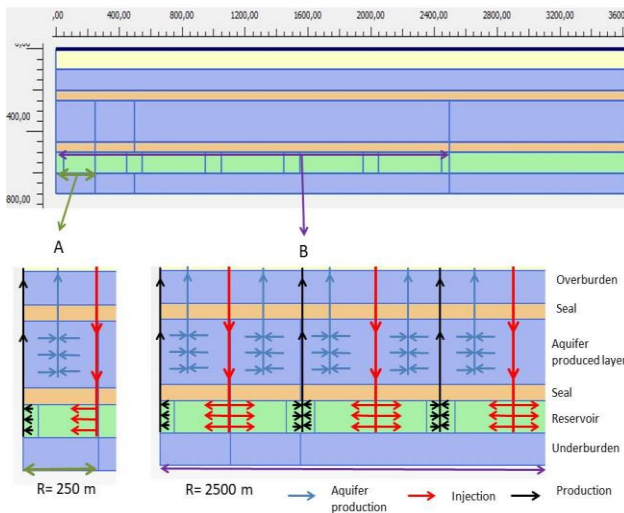


Figure 17: Cross section of A: One injection and one production well, B: Radius of the field: Multiple Production and injection wells

Figure 16 shows the cross section of the four different models for a 100 m thick reservoir. The figure 16 shows the aquifer thickness as follows: A, B, C and D are the 50, 100, 150 and 200 m, respectively. The underburden, the reservoir, the seal of the reservoir, the seal of the aquifer and the top layer in all the models have the same thickness. The difference is only in the second layer (below the sandstone) due to the change in the aquifer layer. In all the models the reservoir depth (500 m) is kept the same to have a fair comparison.

In upper part of figure 17 the cross section of the reservoir is shown. The lower part shows two sections. Figure A shows the injection well and production well with distance of 250 m. Figure B shows the radius of the total reservoir with 2.5 km. In both figures the process of injecting and producing from the reservoir and aquifer are shown. The red line is the injection of the steam in the reservoir. In figure A, the steam has one direction to the production well. In figure B the injection wells have two directions, because on both sides there are a production wells. The black lines indicates the production wells. The production at the edge of the reservoir only comes from one direction. In the middle of the reservoir the production will be from both sides. This is shown with arrows. By applying the pressure increase (5 MPa) in the (large cluster with red arrows) injection part of the reservoir and pressure reduction (1.5 MPa) in the (small cluster with black arrows) production part of the reservoir, the total surface deformation can be calculated. In the second stage (1.2 and 2.2), by producing the aquifer the total deformation- heave due steam injection and subsidence due aquifer production- will be calculated. The production of the aquifer in the second stage is demonstrated with the blue lines. The pressure reduction in the aquifer (clusters with blue arrows) is 1.5 MPa, unless indicated otherwise.

100 m reservoir

This first scenario uses a 100 m thick reservoir. The results of deformation for both tests (single and multiple wells) without modifying the pressure in the aquifer is shown below. Figure 18 shows the deformation with single well and figure 19 shows the deformation by applying multiple wells.

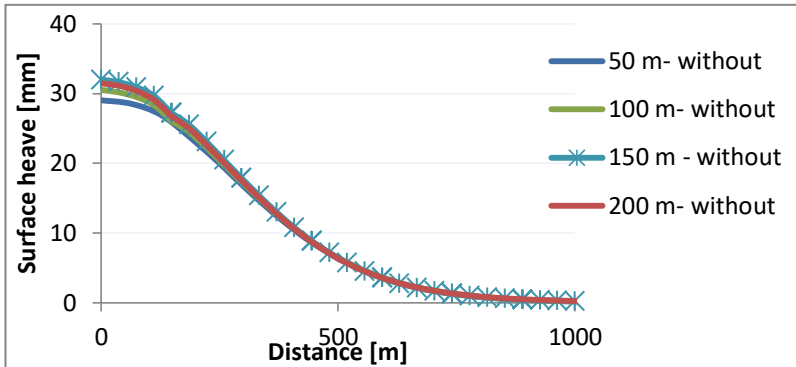


Figure 18: Surface heave due to one injection well and one production well without producing the aquifer applied to four different aquifer thicknesses (α -1.1)

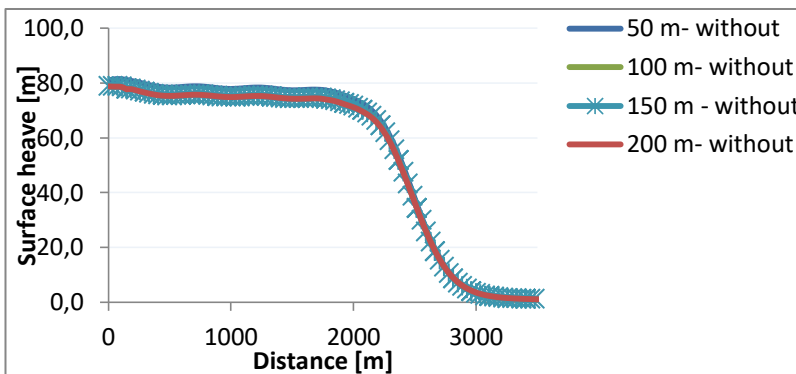


Figure 19: Surface heave due to multiple injection and production wells without producing the aquifer applied to four different aquifer thicknesses (β -1.1)

The results of single well (31 mm) and multiple wells (81 mm) are different. The heave in the multiple wells is almost three times larger than in case of a single well. The effect of subsidence at the surface due to the oil production is very low in both tests. Thus, the heave due the steam injection is dominating the subsidence due compaction causes by oil production. Second difference is in individual heave in the first test and second test. In the first test (α -1.1), each realization has a different heave, but in the second test (β -1.1) all the realizations have the same heave except for the 50 m aquifer. The reason for the difference in deformation in (α -1.1) is, that when the radius of the reservoir is small and the layer above the reservoir is not thick the level of heave will be small. The next steps concern the simulation of the producing the aquifer from the overburden layer (α -1.2 and β -1.2). When producing the aquifer, the pressure drop causes compaction in that specific layer and this can cause subsidence.

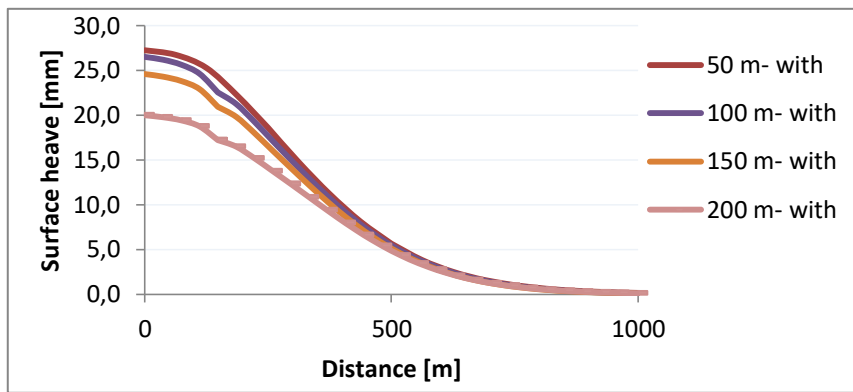


Figure 20: Surface heave due to one injection well and one production well with producing the aquifer applied to four different aquifer thicknesses ($\alpha-1.2$)

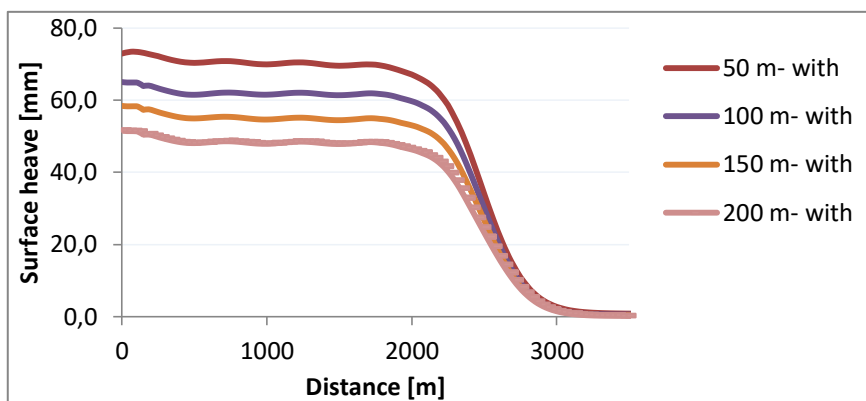


Figure 21: Surface heave due to multiple injection and production wells with producing the aquifer applied to four different aquifer thicknesses ($\beta-1.2$)

The results in figures 20 and 21 show that the level of heave in the case of producing the aquifer is less compared to the level of heave in the case of not producing the aquifer (figures 18 and 19). The aquifer production causes compaction in the aquifer layer which leads to subsidence. This subsidence decreases the level of heave and compensates the resulting deformation at the surface. Where the heave in $\alpha-1.1$ is around 32 mm, the results of producing the aquifer in $\alpha-1.2$ results in a heave between 20 and 27 mm, depending on aquifer thickness. For the large reservoir (multiple clusters, $\beta-1.1$ vs $\beta-1.2$) the differences are larger. The heave for $\beta-1.1$ is 80 mm (figure 19). The results of producing the aquifer ($\beta-1.2$) in figure 12 reduce the heave to 51 and 72 mm, depending on aquifer thickness. The results in figures 20 and 21 show that when the aquifer thickness is larger this results in a larger subsidence, thus lowering the level of heave at the surface. The difference between 50 m (27 mm) and 100 m (26 mm) aquifer is very small. But the difference in 150 (24 mm) and 200 m (20 mm) becomes larger. The results of multiple clusters show a linear difference between the four realizations. Table 3 shows the maximum heave for each aquifer thickness for single/multiple cluster model and the difference without or with producing the aquifer.

Table 3: Maximum heave for different aquifer thickness for single/multiple cluster model

Aquifer thickness (m)	50	100	150	200
α -1.1 (mm)	29	31	32	32
α -1.2 (mm)	27	26	24	20
Difference α (mm)	2	5	8	12
B-1.1 (mm)	81	79	79	79
B-1.2 (mm)	73	65	58	51
Difference β (mm)	8	14	21	28

200 m reservoir:

The second part (2.1 and 2.2), will study the scenario of 200 m thick reservoir. The approach is similar to the 100 m reservoir testes. In this set of experiments, the depth of reservoir starts from 500 m and ends at 700 m. The overburden stays the same in all four different realizations. The layer underneath starts from 700 m and ends at 800 m. I apply the two heave simulations with one cluster and multiple clusters, taking into account the production of the aquifer. The results of the two tests are shown in next figures.

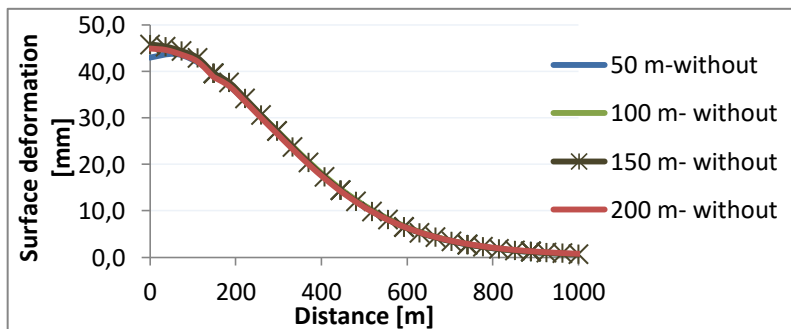


Figure 22: Surface heave due to single injection and single production wells without producing the aquifer applied to four different aquifer thicknesses, for 200 m reservoir

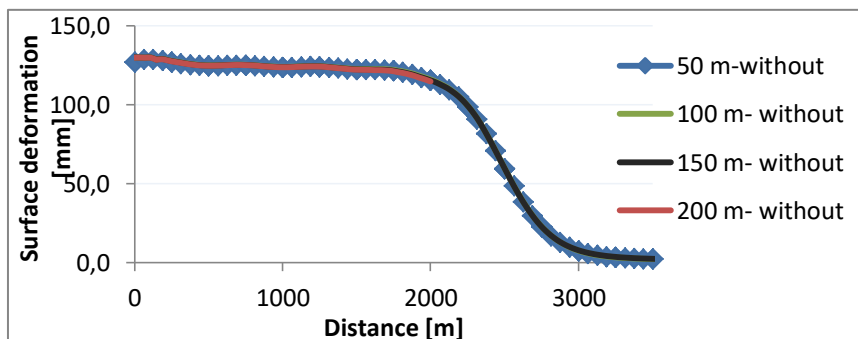


Figure 23: Surface heave due to multiple injection wells and production wells without producing the aquifer applied to four different aquifer thicknesses, for 200 m reservoir

The 200 m reservoir results in larger heave at the surface for small (one cluster) and large (multiple clusters) reservoir comparing to the 100 m reservoir. For the small reservoir (single cluster) the difference is about 15 mm and for the large reservoir (multiple clusters) the difference is about 42 mm. The difference in heave between 100 and 200 m reservoir is caused by increase of pressure in larger interval. The results show that the heave for the

different aquifer thickness is the same and is not affected by the variation of the overburden.

Now, the aquifer will be produced to test compensating effect of the subsidence. The results are shown in the figures 24 and 25. The table below shows the results of 200 m reservoir with the difference in heave when the aquifer is produced (with) and not produced (without).

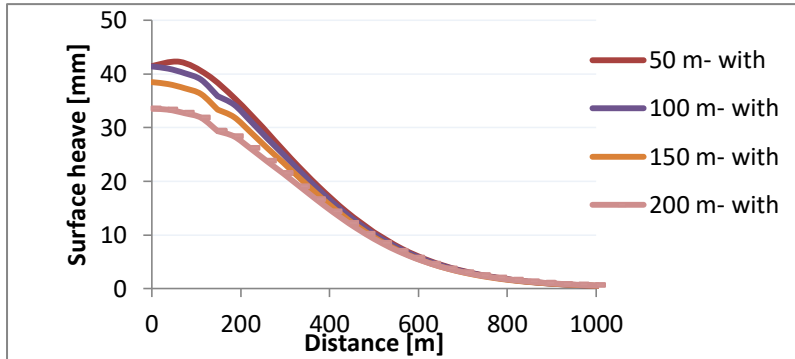


Figure 24: Surface heave due to single injection well and one production well with producing the aquifer applied to four different aquifer thicknesses, for 200 m reservoir

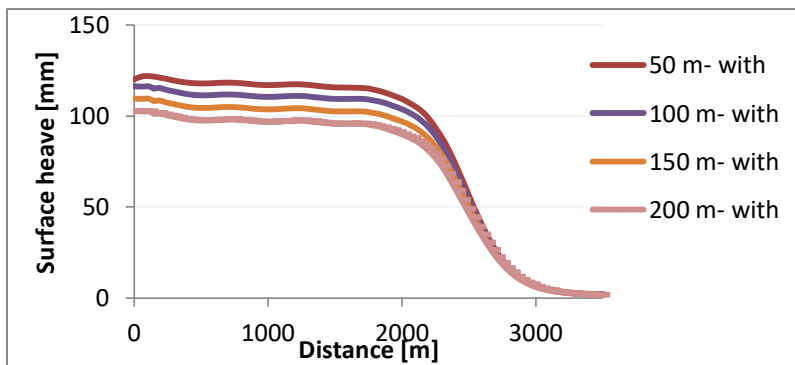


Figure 25: Surface heave due to multiple injection and production wells with producing the aquifer applied to four different aquifer thicknesses, for 200 m reservoir

Table 4: Maximum heave for different aquifer thickness for single/multiple cluster model

Aquifer thickness (m)	50	100	150	200
α -2.1 (mm)	29	31	32	32
α -2.2 (mm)	27	26	24	20
Difference α (mm)	2	5	8	12
B-2.1 (mm)	127	130	130	130
B-2.2 (mm)	120	116	110	102
Difference β (mm)	7	14	20	28

The results of producing the aquifer show that the level of heave is reduced compared to the results when the aquifer is not produced. The level of heave will reduce when the aquifer is large: for 50 m aquifer the heave is 120 mm and for 200 m aquifer the heave is 102 mm. Remarkable point in these two tests (100 and 200 reservoir) is the subsidence level for different aquifer thicknesses. In tables 3 and 4 –“*difference*” row- give for the 100 and 200 m reservoir the same difference. For the 100, 150 and 200 thick aquifer, the differences are 14, 20 and 28 respectively. For 50 m thick aquifer, the two lines are not lie on each other, but the difference is very small. Figures 26 and 27 show the difference of the producing the aquifer for different aquifer and reservoir thicknesses. The terms in the graphs are “OB” the overburden (aquifer thickness), “R” reservoir thickness and “m” the unit meter of the thickness.

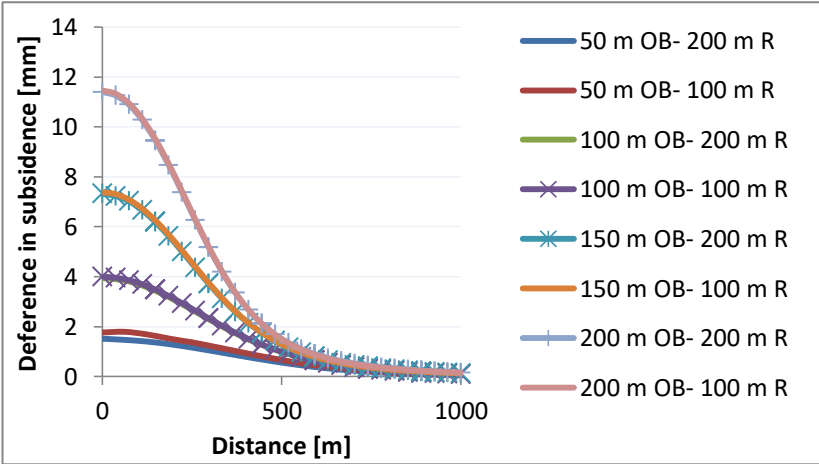


Figure 26: Difference in subsidence for four realizations for 100 m and 200 m reservoir with single injection and single production wells

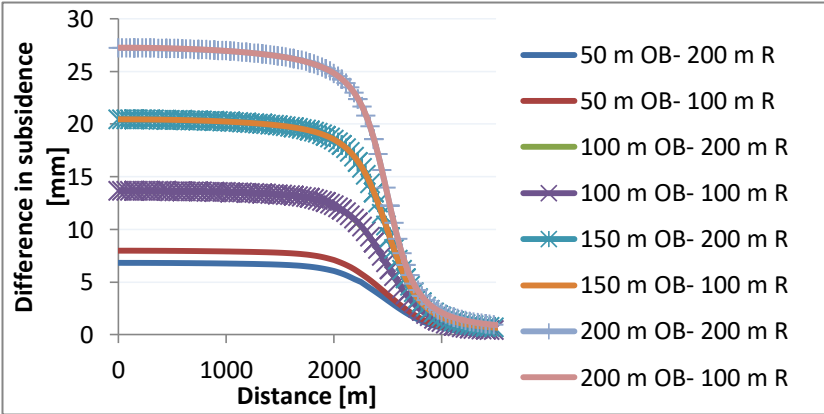


Figure 27: Difference in subsidence for four realizations for 100 m and 200 m reservoir with multiple wells

The figures 26 and 27 show that differences in subsidence of the aquifer layer is independent from the reservoir thickness. So, the change in the reservoir has almost no effect at the aquifer. For the multiple clusters (β) by comparing the effect of subsidence, the difference between 100 m overburden and 150 m overburden is 6.8 mm and between 150 m and 200 m is also 6.8 mm, independent of reservoir thickness. This is not the case for the one cluster (α) deformation. In the one cluster (α): the difference between 100 m and 150 m is 3.4 and between 150 m and 200 m is 4.1. Thus, the level of subsidence due to aquifer production will be the same whatever the reservoir size is. The level of subsidence is depends on the size of the aquifer.

3.3.3 The influence of Pressure in the Reservoir and Aquifer layer

In this part, we will test the pressure differences in the produced aquifer layer and the reservoir. For these tests will used the 100 m thick reservoir and 100 m thick produced aquifer layer (see figure 17-B). These tests will also be applied in the multiple clusters reservoir. In the first test the reservoir pressure is increased with 4, 4.5, 5 and 5.5 MPa respectively. The pressure reduction in the aquifer layer will be 1.5 MPa. The second test is performed by decreasing the pressure in the aquifer layer with 1, 1.5, 2 and 2.5 MPa and keeping the reservoir pressure at 5 MPa. The temperature change stays the same as in previous tests. The results of both tests are shown in the figures 28 and 29.

Table 5: Change in reservoir and aquifer pressure in MPa

	Change A	Change B	Change C	Change D
Reservoir (1)	+4	+4.5	+5	+5.5
Aquifer (2)	-1	-1.5	-2	-2.5

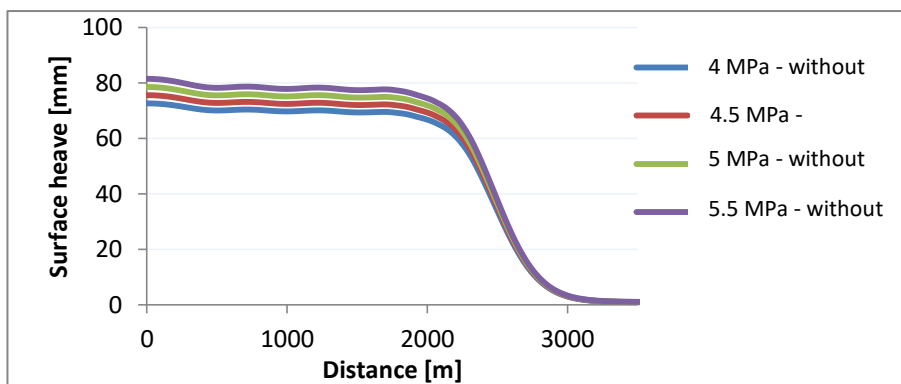


Figure 28: Pressure change in the reservoir, without producing the aquifer

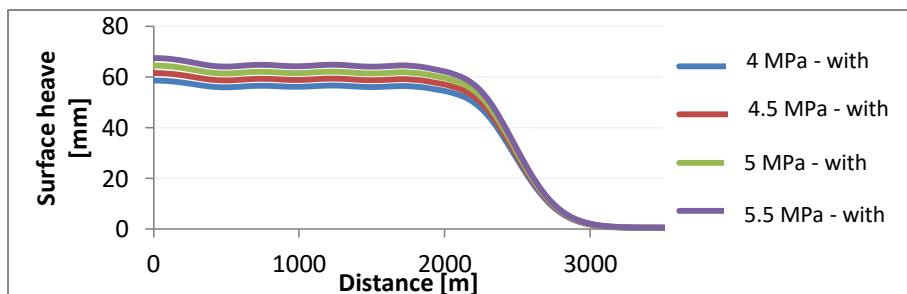


Figure 29: Pressure change in the reservoir, with producing the aquifer

The results in figure 28 show that the heave depends linearly on pressure. The difference in deformation between each pressure-increase is 3 mm. Figure 29 shows the results of producing the aquifer. The pressure reduction in aquifer layer is for all four tests the same. The subsidence due to production in the aquifer layer has a value of 14 mm.

Figure 30 shows the results by varying the pressure change in the aquifer layer.

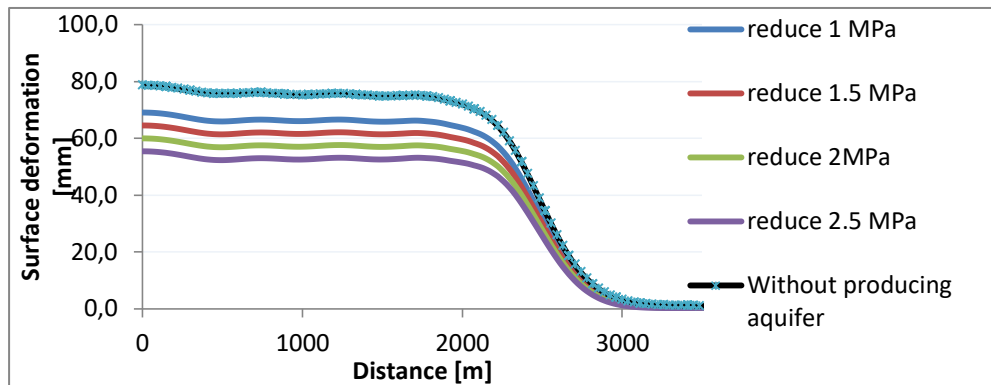


Figure 30: Different pressure decrease in the aquifer layer

Figure 30 shows the effect of deformation caused by pressure reduction in the aquifer layer. The black line (without producing aquifer) is the total heave at the surface. The other lines show the subsidence due to aquifer production caused by different pressure reduction. The results show a constant subsidence by each pressure reduction. This means, by reduction of each 0.5 MPa, leads to a subsidence of 4.5 mm at the surface.

3.4 Sensitivity

In this part, we will test the change of the two elasticity parameters, the Young's modulus and Poisson's ratio. This will be done for the reservoir rock and for two overburden rock types, the limestone and the shale. These sensitivity tests will be applied on 100 m reservoir and 100 m aquifer layer, figure 17-B. The pressure and temperature change is the same for all the tests. In the figures, the results of producing the aquifer are provided. The third part in this chapter provide the results for varying the Young's modulus, the reservoir thickness and pressure increase as well as the variations of these quantities in the aquifer. The last part, consists of small studies by testing the compensate of heave by subsidence, maximum pressure increase, thermal expansion.

3.4.1 Reservoir

There are six different tests performed to understand the influence of Young's modulus and Poisson's ratio in the reservoir. The first three of the tests are performed by changing only the Young's modulus. The three different values are 20, 40 and 60 GPa [18] and the Poisson's ratio for these tests is 0.2. Two tests will be performed by changing only the Poisson's ratio by 0.25 and 0.3. The Young's modulus is kept 13 GPa. The last test is done by taking the extreme value of Young's modulus 60 GPa and Poisson's ratio 0.3. The results of the tests are shown in the next figures. In these figures is also the graph for the base case (Young's modulus = 13 GPa and Poisson's ratio = 0.2) plotted. The letters E and V in the figures are referred to Young's modulus and Poisson's ratio, respectively.

Table 6: Varying Young's modulus and Poisson's ratio in the reservoir

	Change A	Change B	Change C	Change D	Change E	Change F
Reservoir (1)	E20- V0.2	E40- V0.2	E60- V0.2	E13- V0.25	E13- V0.3	E60- V0.3

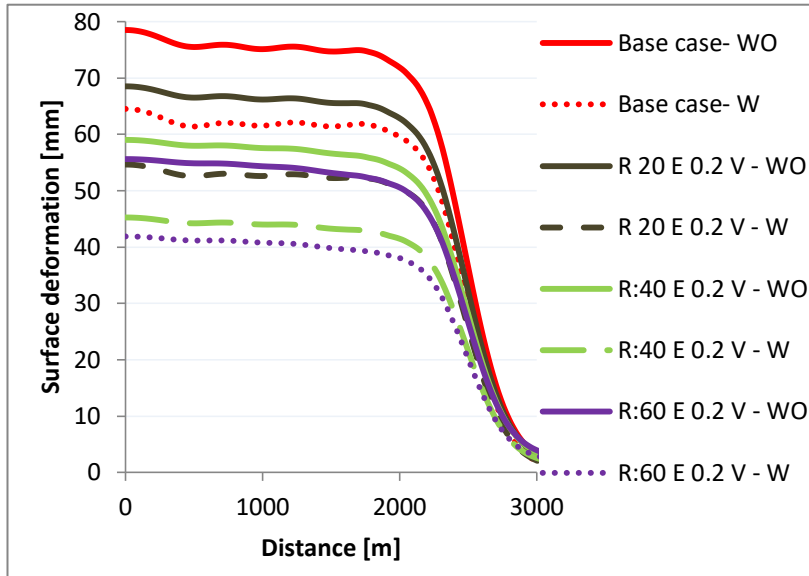


Figure 31: Varying the Young's modulus in the reservoir. The solid lines: without producing the aquifer, the dashed lines: without producing the aquifer

The results of deformations are very different as it shown in figure 31. The heave will be lower when the Young's modulus is higher. For 13 GPa Young's modulus, the heave is 80 mm. By changing the Young's modulus to 20, 40 and 60 GPa, the heave will be 69, 59 and 55 mm, respectively. Second effect of increasing the Young's modulus is the smoothness of the deformation line. The curve-effects in the lines (Base case and R20) are caused by the production of hydrocarbons in the reservoir, since I take into account the effect of hydrocarbon producing in the simulation. The increase in Young's modulus means higher stiffness in the rock. By comparing the heave without (WO) and with (W) aquifer produced layer, the difference is the same for the three models, 14 mm.

Figure 32 shows the results by varying the Poisson's ratio. Table 5 shows the maximum deformation by varying Young's modulus and Passion ratio in the reservoir for the WO case.

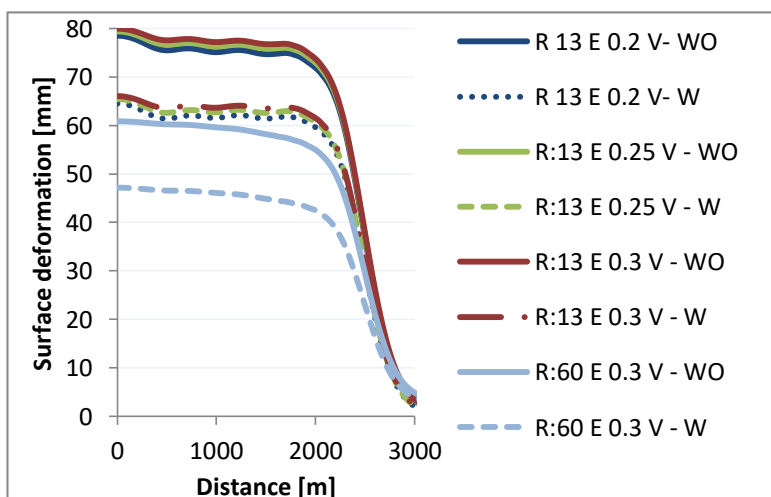


Figure 32: Varying Poisson's ratio in the reservoir. Solid lines: without producing aquifer, dashed lines: with producing the aquifer

Table 7: Maximum deformation (mm) by varying Young's modulus and Poisson's ratio for WO

		V		
		0,2	0,25	0,3
	BC	78,5	79,4	80
E	20 (GPa)	68,5	70,1*	71,7*
	40 (GPa)	59	61,3*	63,8*
	60 (GPa)	55,6	58,1	60,9

Table 7 shows the maximum deformation by variation of Young's and ratio in the reservoir from figure 30 and 31. This table clarifies the effect of Young's modulus and Poisson's ratio on the deformation. The maximum deformation difference of variation for Poisson's ratio (between 0,2 and 0,3) is 5 mm when the Young's modulus is 60 GPa. Below this value of Young's modulus the difference will be around 2 mm, this is also shown in table 7. This table also clarifies the effect of Young's modulus for the deformation. As it has been mentioned before, the heave will be less when the Young's modulus is high. The heave difference in the cases without (WO) and with (W) production of the aquifer is similar to the base case, 14 mm. The difference between not producing (WO) and producing (W) the aquifer by increasing the Young's modulus to 60 GPa and the Poisson's ratio to 0.3 also stays the same, 14 m. Note the effect of Young's modulus: the level of heave will be higher when Young's modulus is low. But this has no effect on subsidence in the aquifer. The level of subsidence in the aquifer stays the same even when the Young's modulus in the reservoir is high. The effect of Poisson's ratio is very small (high Young's modulus) or negligible (low Young's modulus).

3.4.2 Overburden

In this part, we will test the sensitivity of two types of rock in the overburden. The two rock types are the shale (= seals) and the limestone (= aquifer). The shale will be tested because of the deposit above the reservoir and aquifer layer. The limestone is chosen because the aquifer is produced from this layer. The tests will be as follow: take two higher values for Young's modulus for the shale and limestone and keep the Poisson's ratio fixed. Then use the highest value for Young's modulus and take 0.3 for Poisson's ratio. The last part will be done by taking the maximum values for the reservoir (E = 60 GPa and $\nu=0.3$) and for the specific layer. The Young's modulus for the shale will be increased by 10 and 15 GPa and for the limestone will be 30 and 50 GPa. The Poisson's for limestone and shale will be changed by 0.3. Here will also be tested the level of heave for producing the aquifer (W). Figure 33 shows the results for shale and figure 34 shows the results of limestone by varying the elastic properties for both layers individually.

Table 8: Varying Young's modulus and Poisson's ratio for the shale (seal) and limestone (aquifer)

	Change A	Change B	Change C	Change D
Shale (1)	E10- V0.2	E15- V0.2	E15- V0.3	R:E60- V0.3 and S:E15- V0.3
Limestone (2)	E30- V0.2	E50- V0.2	E50- V0.3	R:E60- V0.3 and S:E50- V0.3

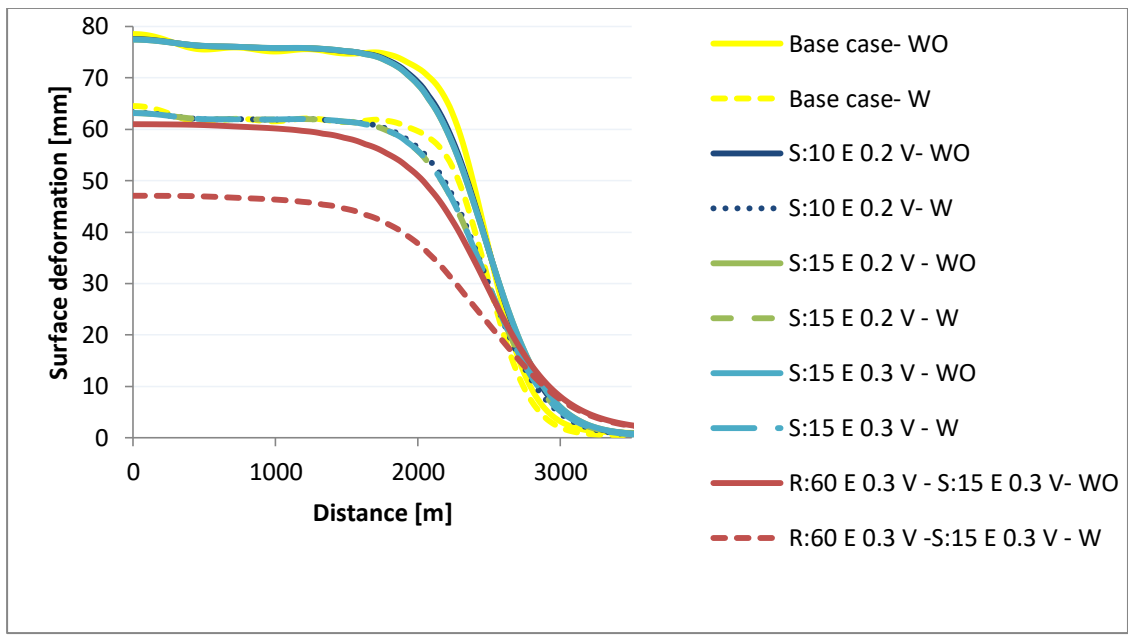


Figure 33: Varying Young's modulus and Poisson's ratio in the shale layers (seals).

From the results in figure 32 is clear that the shale has very low effect at the deformation. This has two reasons. The first reason is because of the small thickness of the shale layer compared to other layers. The second reason is the low values of Young's modulus for this type of rock. The difference between producing and not producing the aquifer stays the same as the base case. The results of the 60 and 15 GPa Young's modulus for the reservoir rock and seal, respectively, (red dotted and red straight line) are low comparing to other lines because of the high Young's modulus value in the reservoir. The high stiffness in the reservoir causes lower heave at the surface. In this test is the difference between producing and not producing the aquifer the same as the base case, 14 mm.

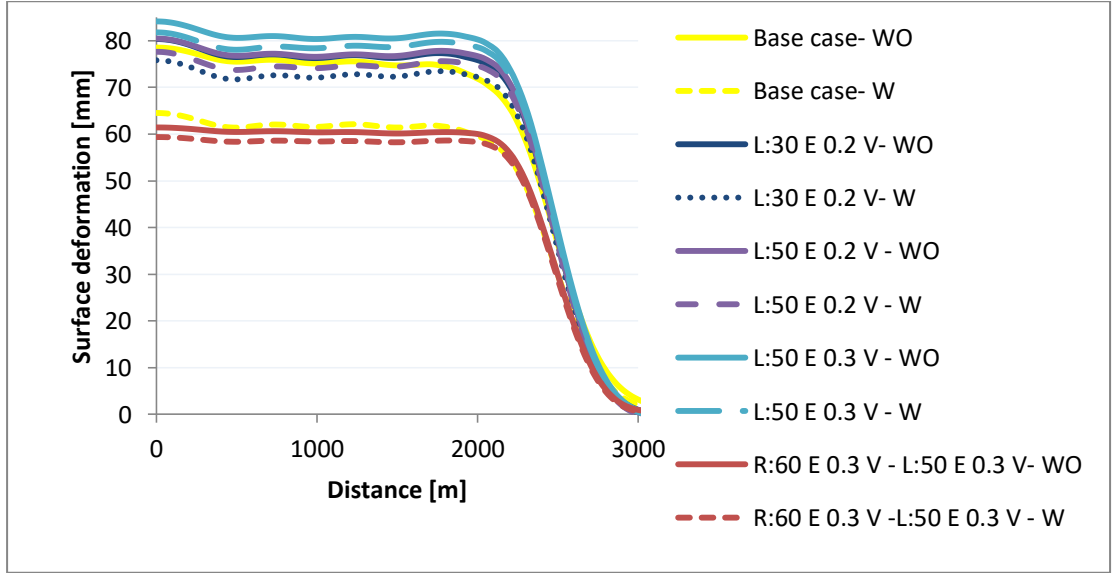


Figure 34: Varying Young's modulus and Poisson's ratio in limestone (aquifer).

The results for the WO are almost the same by varying the Young's modulus and Poisson's ratio. The difference in the base case and the largest deviation (when the Young's modulus is 50 GPa) is 5 mm. The reason for this small deviation is that the change is applied in the overburden of the reservoir. The deviation in results is larger when the production of the aquifer is applied in the model. For the base case is the result for W 64 mm and for the other tests are the results between 76 and 82 mm. Thus the effect of subsidence due to producing the aquifer will be very low when the Young's modulus is very high in this layer. The effect of Poisson's ratio is very small for the deformation as in earlier tests. The results of the maximum deformation due to variation of E and ν are shown in the tables below.

Table 9: Maximum deformation (mm) for the aquifer						
WO		W		WO-W		
V		V		V		
	0,2	0,3	0,2	0,3	0,2	0,3
BC	78,5	80	64,5	66,1	14,0	13,9
E 30 (GPa)	80,4	83,9 ⁵	75,8	80,2 ⁴	4,6	3,7 ⁴
50 (GPa)	80,4	84,1	77,6	81,8	2,8	2,3

3.4.3 3D Plots for Reservoir and Aquifer

In this part, we will test the deformation by varying the Young's modulus for different reservoir and aquifer thicknesses. The Young's modulus varies from 10 to 60 GPa for reservoir layer and 10 to 50 GPa for aquifer layer. The thickness varies from 50 to 200 m. The 3D plots give an indication how the deformation relates to Young's modulus and thickness of the layer. As it has been mentioned before [18], the Young's modulus in one layer is not a fixed value, but it varies. With the obtained parameters as pressure increase in the reservoir, reservoir thickness and heave at the surface will this figure provides a good average estimate of the Young's modulus. First 3D plot shows the maximum deformation with increase of pressure by 3, 4 and 5 MPa. Also, the effect of deformation due to producing the aquifer is given in figure 35-B.

Increase reservoir pressure

- 1= 5 MPa
- 2= 4 MPa
- 3= 3 MPa

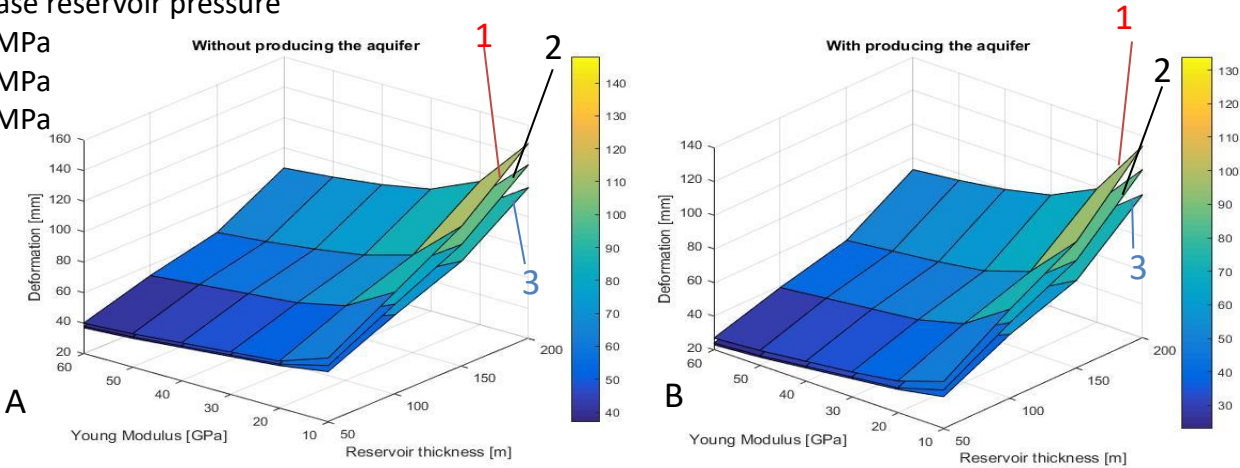


Figure 35: 3D plot of maximum deformation by varying Young's modulus, reservoir thickness and pressure increase. A) Without producing the aquifer. B) With producing the aquifer.

⁵ These results are not plotted in the graphs.

The results from figure 35 show that the lowest level of heave at the surface is when the reservoir thickness is 50 m in combination of high Young's modulus, 40 mm (5 MPa) and 37 mm (3 MPa), respectively. The opposite gives a large heave, when the reservoir is 200 m thick and the Young's modulus is 10 GPa, 148 and 119 mm for 5 and 3 MPa, respectively. From the three pressure change, when the Young's modulus is 30 GPa or higher (till 60 GPa) the deformation behaves almost linear. The level of heave become smaller and smaller in constant steps. The difference in level of heave is in this region (between 30 and 60 GPa) for all the thicknesses almost 15 mm. The heave increases very fast when the Young's modulus is between 10 and 25 GPa for all the thicknesses. The difference between producing and not producing the aquifer stays the same for all the different reservoir thickness and Young's modulus, 14 mm. Thus, the thickness and Young's modulus variation does not change the effect of producing the aquifer. But the heave behavior is not linear by variation Young's modulus.

The next 3D figure shows the deformation by variation the Young's modulus and thickness in the aquifer layer. In this figure only the deformation due to aquifer production is shown. As we tested before in chapter 3.4.2, the heave stays the same, when the Young's modulus or the thickness is varied.

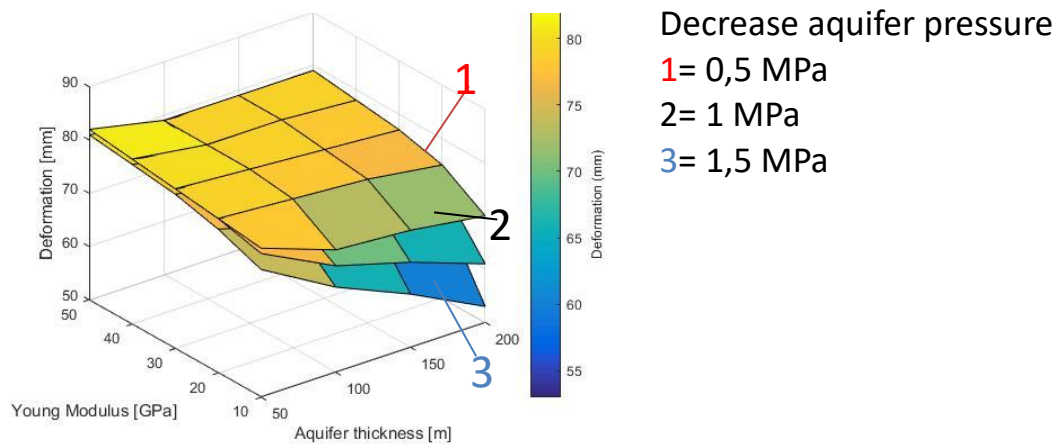


Figure 36: 3D plot by varying Young's modulus, thickness and pressure reduction in the aquifer.

Figure 36 shows that the level of heave at the surface decreases when the aquifer thickness is large and Young's modulus is low. When the aquifer is 200 m and Young's modulus is 10 GPa, the level of heave decreases to 53 mm by pressure reduction of 1.5 MPa in the aquifer. The opposite (the aquifer thickness is small and the Young's modulus is high) will have no effect to decrease the level of heave. Also, when the aquifer thickness is large, but the Young's modulus is high (between 50 and 30 GPa) the decrease in level of heave will be very small. So, the heave will not compensate by subsidence when the Young's modulus is very high, even when the aquifer is large.

3.4.4 Extra research

In this part, we do three small tests by (1) investigating the turning point of the heave, (2) varying thermal expansion and (3) investigating at which pressure increase the fracture will happen.

(1) Compensation of heave by subsidence

It is important to understand in which conditions the heave due to steam injection and subsidence due to aquifer production cancel each other. Whereby the deformation at the surface will be almost zero. For this test, the thicknesses for the reservoir and aquifer are 100 and 200 m respectively. The reservoir depth is at 500 m (see figure 16-D). The Young's modulus for the reservoir and aquifer are 60 and 7 GPa respectively. The pressure increase in the reservoir is 5 MPa and the pressure reduction in the aquifer is 2 MPa. The result of total heave at the surface for this test was almost zero (0.3 mm). The 0.3 mm indicates that there is no deformation at the surface.

(2) Thermal expansion

Thermal expansion is a rock property that determines the level of expansion of rock due to increase of temperature. This expansion leads to increase the level of heave. For the next tests, the 100 m thick reservoir and aquifer is used. The reservoir depth is at 500 m (see figure 16-B). The pressure increase in the reservoir is 5 MPa. The pressure reduction in the aquifer is 1.5 MPa. Both pressures kept fixed during the different tests. Only the thermal expansion is varied. Next table shows the variation in thermal expansion and the results of maximal deformation at the surface. The effect of producing the aquifer is also tested (W). The last column is the difference between without producing and with producing the aquifer.

Table 10: Thermal expansion

Thermal expansion [K ⁻¹]	Deformation [mm]		Difference [mm]
	WO	W	
0,7*10 ⁻⁶	79	65	14
0,95*10 ⁻⁶	89	75	14
2*10 ⁻⁶	130	116	14
5*10 ⁻⁶	208	194	14

From the results, there are three remarkable points. The first point, the difference between WO and W is 14 mm. This means that the thermal expansion has no effect at producing the aquifer. The decrease of heave at the surface due to the aquifer production stays the same. Secondly, the level of heave does not increase constantly by constant increase of the value of thermal expansion.

(3) Fracture

The hydrocarbons are trapped in a reservoir below the seal. This seal has to be intact without creating any crack or fraction. This lead to leak of hydrocarbon and reduction of pressure in the reservoir. By increasing the pressure above the limited pressure, this may cause fractures in the reservoir but also in the seal⁶. To avoid this issue, the pressure increase has to be under control. Table 11 shows the results by varying the tension strength and Young's modulus.

Table 11: Maximal pressure increase to before creating fractures

Maximal pressure increase without failure [MPa]	Tension strength (cut off) [MPa]	Young's modulus [GPa]
17	5	13
17,5	5	20
17	5	40
22,5	10	13
22	10	40

The results show that by increase of Young's modulus, the maximum pressure before creating fracture will be the same. On the other hand, by increase the tension strength, the rock can handle higher pressure before creating fracture in the subsurface. For all the tests, the fracture happens directly below the seal, see appendix E.

⁶) Lecture of Peter Schutjens (Geomechanics at Shell): the risk is high in the seal to create fracture due to injection in the reservoir, see appendix E.

4 Discussion

We will discuss four points in this part: (1) the importance of data from one field, (2) the assumption of a flat reservoir, (3) the used Young's modulus and (4) fractures and isotropic for thermal expansion in the reservoir. (1) Creating a model without using data from one specific field is like a "religious" method. The decisions are based on "faith" and the results are difficult to check. This is in general the case of simulation models without using real data from a specific field. But we hope that this may be a step to help the other deformation researchers to use this and develop their investigation. It is difficult to use parameters that we cannot provide from a field or using values from literature. (2) Secondly, the reservoir is assumed to be flat. The reality shows that the most hydrocarbons are trapped in an anticline or tilted reservoir. The results of deformation in an anticline or tilted reservoir can be different than from a flat reservoir. Since the pore pressure increase in the reservoir creates force that has direction perpendicular to the surface of the reservoir layer. (3) The third point is the elastic property, Young's modulus. From [18] is known that one layer has different Young's modulus. This can vary from 11 to 60 GPa. For modeling a reservoir with such a large difference values make the tests difficult. It is difficult to use all this values to estimate the level of heave. But it is possible to use the level of heave to estimate the average value for the Young's modulus. (4) Last but not least, the presence of fractures and the isotropic thermal expansion factor in the reservoir may change the deformation. We assumed that we do not have fractures and the reservoir is isotropic for thermal expansion. The existence of fracture/fault can create another dimension of expansion in the reservoir. This can lead to an expansion perpendicular to the plane of fault. So, will this expansion in the fracture/fault, have an influence at the heave in the surface direction? And will the thermal expansion then be isotropic?

5 Conclusion

Steam injection is an EOR technique which creates heave at the surface. In this research a 2D model is created in Plaxis, to investigate the effects of changing three properties to simulate the effect on the heave at the surface caused by the steam injection. The three properties are the reservoir thickness, the pressure increase caused by steam injection and the elastic properties.

The results in this research show that when reservoir thickness is increased, the heave at the surface will increase. The effect of increasing the pressure cause, just like reservoir thickness, also increases the heave.

The effect of the elastic properties, Young's modulus and the Poisson's ratio, on the heave is investigated. The Poisson's ratio does not show a significant change in heave. While, increasing the Young's modules shows a decrease in heave caused by steam injection.

The aquifer above the reservoir is produced to compensate the heave caused by steam injection. Production in the aquifer will cause subsidence and therefor can compensate the heave. This subsidence is not depended on the reservoir conditions, this means that the heave caused by the steam injection in the reservoir and subsidence by the aquifer are not coupled. However, changing the thickness, pressure drop and Young modulus of the aquifer have influence on the level of subsidence. With an increase in aquifer thickness and/or pressure the subsidence level increase. With an increase in Young's modulus of the aquifer, the subsidence level decreases.

6 Future work

As discussed, a 2D model of the field is created to get a better understanding of the effect of steam injection in the reservoir and at the same time aquifer production on heave at the surface. The following recommendations could be used to investigate the heave level for more realistic scenarios. Firstly, as mentioned in the discussion, use of realistic reservoir data and shape. Also taking into account the porosity and permeability changes. Secondly, the effect of present fractures/faults in the reservoir and aquifer. Furthermore, creating a 3D field instead of 2D model.

References

- [1] Geertsma, J. "Land subsidence above compacting oil and gas reservoirs": SPE 3730 1973
- [2] Wong, R.C.K., Lau, J., University of Calgary, "Surface Heave Induced by Steam Stimulation in Oil Sand Reservoirs": Journal of Canadian Petroleum Technology, January 2008, Volume 47, No. 1
- [3] Penney, R., Baqi Al Lawati, S., Hinai, R., van Ravesteijn, O., Rawnsley, K., Putra, P., Geneau, M., Ikwumonu, A., Habsi, M., and Harrasy, H., "First Full Field Steam Injection in a Fractured Carbonate at Qarn Alam, Oman", SPE 105406, 2007
- [4] Lisowski, M., "Analytical volcano deformation source models": Chapter 8
- [5] Teatini, P., Gambolati, G., Ferronato, M., Settari, A., Walters, D.: "Land uplift due to subsurface fluid injection": Journal of Geodynamics 51 (2011) 1–16
- [6] Koros, W., O'Sullivan, J., Pogacnik, J., O'Sullivan, M., and Ryan, G., "Comparison of Coupled One-Dimensional Subsidence Models": Proceedings World Geothermal Congress 2015
- [7] Xu, J., Wu, Z.,: "Tubular string characterization in high temperature high pressure oil and gas wells" 2014
- [8] Nanayakkara, A.S., Wong, R.C.K., : "How Far does Surface Heave Propagate?": KSCE Journal of Civil Engineering (2009) 13(4):297-303
- [9] Dake, L.P.,: Fundamentals of reservoir engineering: 1998
- [10] Macaulay, R.C., Krafft, J.M., Hartemink, M., Escovedo, B.,: "Design of a Steam Pilot **In A** Fractured Carbonate Reservoir", · Qarn Alam Field, Oman: SPE 30300 1996
- [11] Shahin, G.T., Moosa, R., Kharusi, B., Chilek, G.,: "The physics of steam injection in fractured carbonate reservoir, engineering development options that minimize risk." SPE 102186: September 2006
- [12] Bakker vd, H. Mudde, R.: "Fysische transportverschijnselen": 3^e druk 2008
- [13] Wright, T.J.: "Matlab file Mogi" University of Leeds , 12 August 2009
- [14] Pollard, D.D., Fletcher, R.C., "Fundamentals of structural geology" first publication: 2005
- [15] "Plaxis 2D References manual", Plaxis bv Delft "2016"
- [16] reservoir engineering course: AES1340, 2016
- [17] Bakhorji, A., "Velocity of P- and S-Waves in Arab-D and WCSB Carbonates: AAPG Search and Discovery Article #90170©2013 CSPG/CSEG/CWLS GeoConvention 2008, Calgary, Alberta, Canada, May 12-15, 2008
- [18] Reza Najibi, A., Ghafoori, M., Reza Lashkaripour, G., Reza Asef, M., "Empirical relations between strength and static and dynamic elastic properties of Asmari and Sarvak limestones, two main oil reservoirs in Iran": Journal of Petroleum Science and Engineering 126(2015)78–82
- [19] Eppelbaum, L., Kutasov, I., Pilchin, A.,: " Applied Geothermics" : chapter 2 "Thermal Properties of Rocks and Density of Fluids" pages: 99-149
- [20] Robertson, E.C "Thermal properties of rock" 1988
- [21] The university of Texas at Austin: "Some useful numbers on the Engineering properties of materials (Geologic and otherwise)" GEOL615

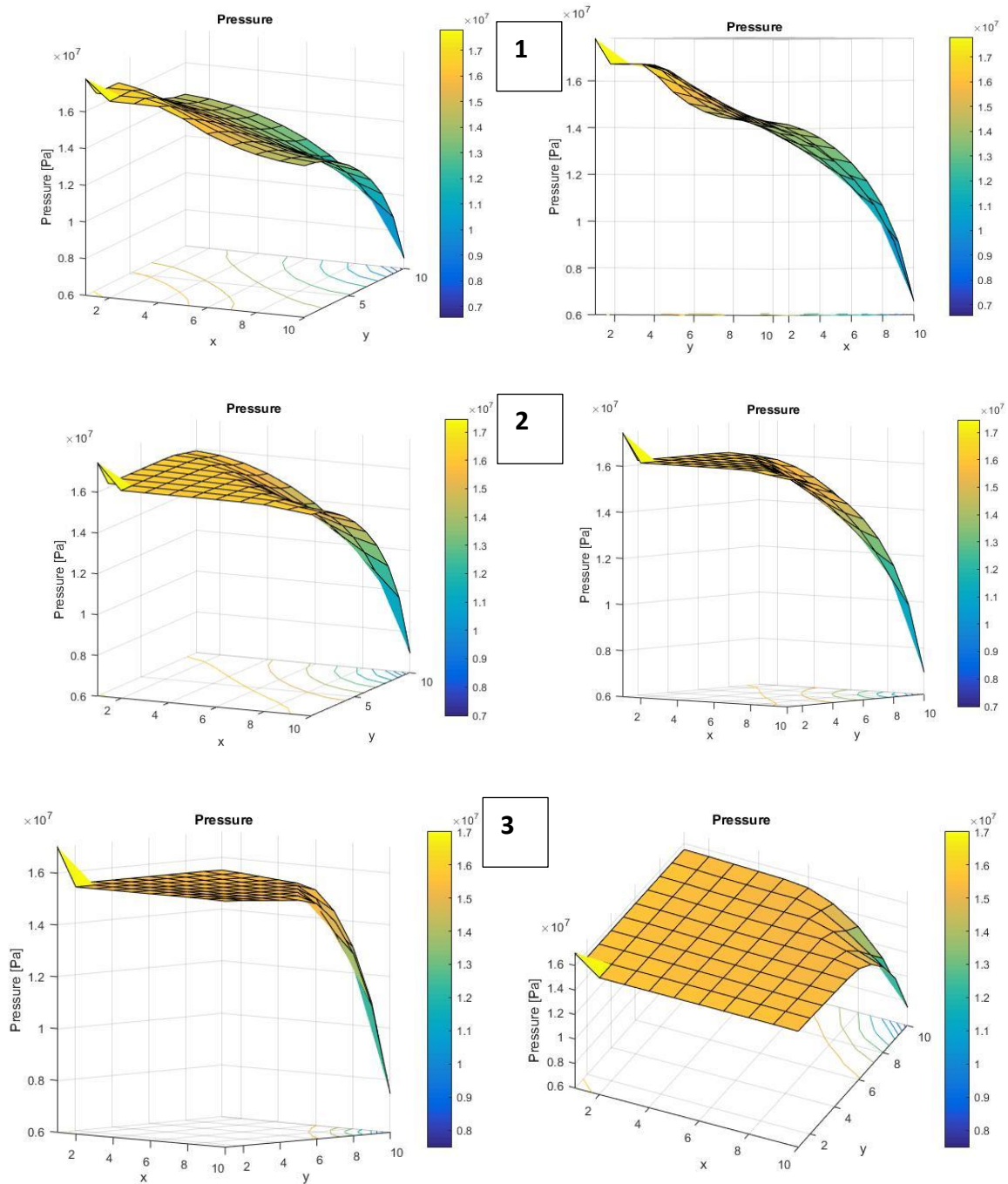
Appendix A –

The used table for creating Geertsma model.

TABLE 1—VALUES OF $A = R \int_0^{\infty} J_1(\alpha R) J_0(\alpha r) e^{-\nu a} d\alpha$ FOR RANGES OF VALUES OF $\rho = r/R$ AND $\eta = D/R$

ρ	η											
	0.0	0.2	0.4	0.6	0.8	1.0	1.2	1.4	1.6	1.8	2.0	3.0
0.0	1.0000	0.8039	0.6286	0.4855	0.3753	0.2929	0.2318	0.1863	0.1520	0.1258	0.1056	0.0513
0.2	1.0000	0.7983	0.6201	0.4771	0.3683	0.2876	0.2279	0.1835	0.1500	0.1244	0.1045	0.0510
0.4	1.0000	0.7789	0.5924	0.4508	0.3473	0.2720	0.2167	0.1754	0.1442	0.1202	1.1014	0.0502
0.6	1.0000	0.7349	0.5377	0.4043	0.3124	0.2470	0.1989	0.1628	0.1351	0.1135	0.0965	0.0488
0.8	1.0000	0.6301	0.4433	0.3368	0.2658	0.2147	0.1762	0.1465	0.1234	0.1049	0.0901	0.0470
1.0	0.5000	0.3828	0.3105	0.2559	0.2130	0.1787	0.1510	0.1286	0.1102	0.0951	0.0827	0.0449
1.2	0.0000	0.1544	0.1871	0.1795	0.1621	0.1433	0.1257	0.1103	0.0965	0.0848	0.0748	0.0424
1.4	0.0000	0.0717	0.1101	0.1216	0.1197	0.1120	0.1024	0.0925	0.0831	0.0744	0.0667	0.0398
1.6	0.0000	0.0400	0.0682	0.0829	0.0876	0.0865	0.0824	0.0768	0.0707	0.0646	0.0589	0.0370
1.8	0.0000	0.0249	0.0449	0.0580	0.0647	0.0668	0.0659	0.0633	0.0597	0.0557	0.0516	0.0343
2.0	0.0000	0.0168	0.0312	0.0418	0.0485	0.0519	0.0528	0.0520	0.0502	0.0477	0.0450	0.0315
3.0	0.0000	0.0042	0.0082	0.0118	0.0149	0.0174	0.0193	0.0207	0.0216	0.0221	0.0222	0.0198

Appendix B –

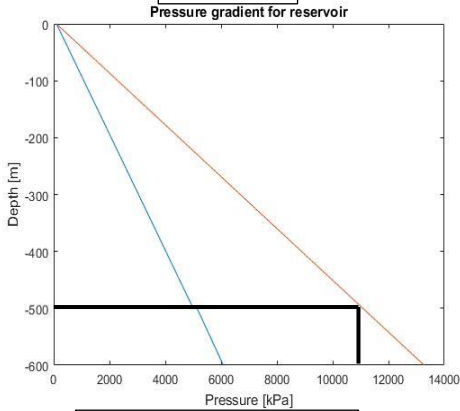


In these figures, three different time steps are shown. Each figure shows how the pressure increase is propagating due to injection in the reservoir. Figures 1 show the begin stage of injection. Figures 2 show the second stage, the injection reaches the middle of the reservoir. Figures 3 show the last stage.

Appendix C –

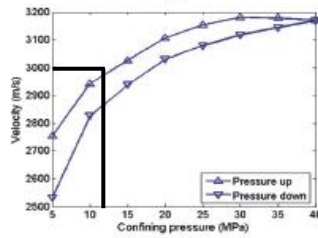
Choosing Young's modulus

1^e step



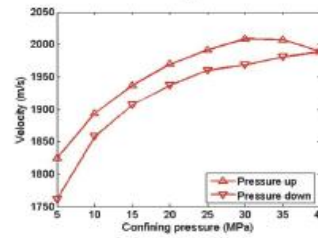
Confining pressure: 11 MPa

P-wave



2^e step

S-wave



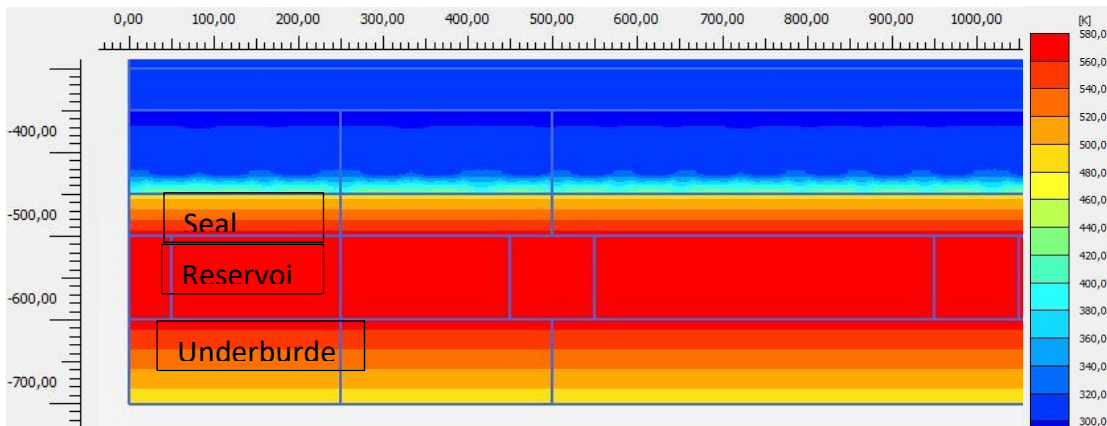
P-wave velocity: 3000 m/s

3^e step

Sample ID	V _p (km/s)	V _s (km/s)	Density (g/cm ³)	UCS (MPa)	E _c (GPa)
1	5.381	3.073	2.60	178.2	46.2
2	4.876	2.712	2.46	122.4	34.3
3	5.737	3.102	2.60	175.9	48.1
4	5.951	3.261	2.70	176.9	53.3
5	4.809	2.797	2.30	81.90	31.0
6	5.189	2.893	2.60	100.7	36.4
7	2.690	1.703	2.60	31.90	11.4
8	4.887	2.809	2.30	68.00	28.8
9	3.170	1.981	2.40	50.20	13.9
10	4.831	2.942	2.70	153.8	34.0
11	4.036	2.691	2.62	105.3	24.9
12	2.826	1.884	2.43	41.50	10.9
13	3.924	2.337	2.40	74.00	18.2
14	3.691	2.045	2.35	34.10	13.3
15	3.600	2.400	2.61	63.80	17.1
16	3.229	2.123	2.50	56.50	12.7
17	3.694	2.44	2.53	58.20	16.7
18	4.373	2.405	2.41	53.50	17.3
19	3.454	2.281	2.59	50.80	14.0
20	3.445	2.261	2.61	59.40	13.3
21	3.663	2.419	2.44	40.90	12.2
22	3.696	2.012	2.54	33.60	7.90
23	3.746	2.475	2.59	48.00	10.0
24	3.852	2.608	2.63	74.50	12.8
25	4.221	2.488	2.62	70.80	7.80
26	3.353	2.357	2.54	75.90	13.4
27	2.381	1.587	2.47	33.80	7.1
28	3.855	2.461	2.63	47.50	13.4
29	3.935	2.644	2.58	78.60	14.5
30	6.480	3.288	2.70	180.0	90.0
31	4.063	2.719	2.60	72.60	16.8
32	4.854	2.880	2.69	118.0	24.4
33	4.274	2.794	2.65	122.0	22.6
34	4.854	2.880	2.69	118.0	24.4
35	5.707	3.149	2.70	157.3	66.0
36	5.016	3.108	2.70	148.2	51.0
37	5.744	3.206	2.70	143.7	66.0
38	4.185	2.690	2.40	91.40	19.5
39	3.834	2.368	2.10	25.10	17.4
40	3.064	1.963	2.30	28.15	4.70
41	3.877	2.418	2.30	46.80	11.5
42	3.690	2.430	2.70	54.70	13.0
43	3.77	2.44	2.60	56.50	22.5
44	4.072	2.618	2.60	75.40	12.0
45	5.689	3.289	2.70	171.1	50.7

Choosing Young's modulus: 13 GPa

Heat Loss Distribution in Plaxis



Appendix D –

The used parameters in Plaxis

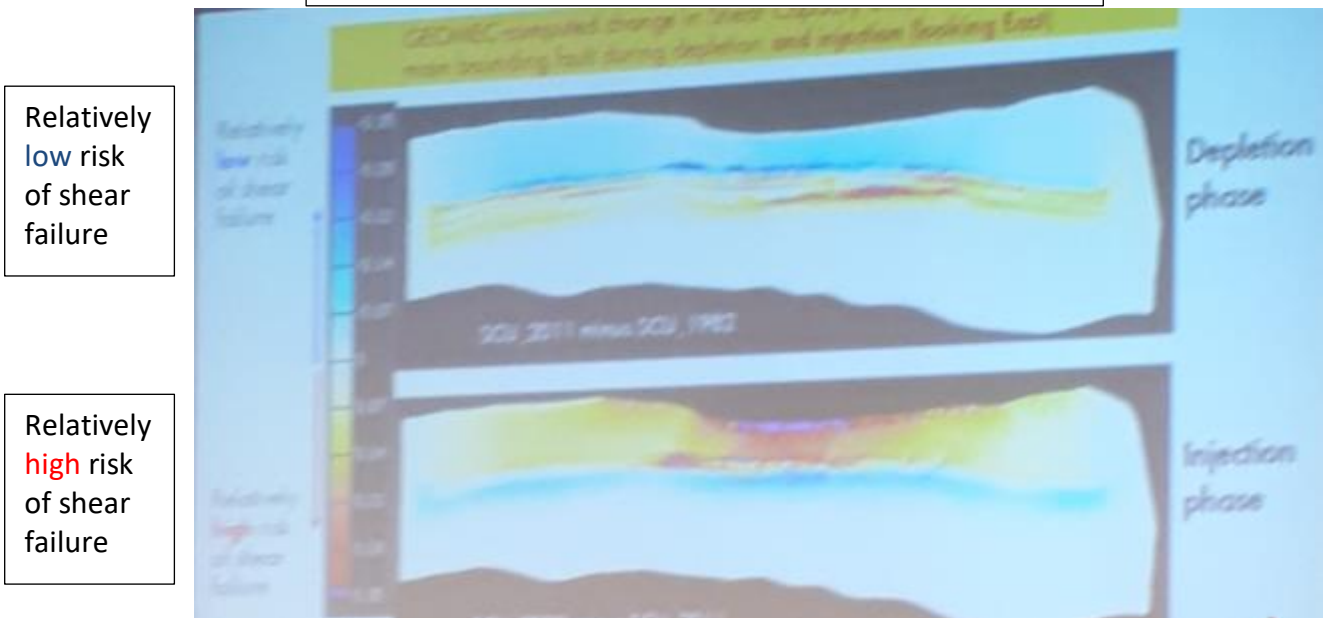
Rock parameters	E (GPa)	ν (-)	ρ (g/cm ³)	ϕ (-)	e initial	C(kJ/t/K)	λ (W/m/K)	$\alpha(1/K)*10^{-6}$	$\phi''(Kw/m^2)$	Tensile (MPa)
Reservoir rock	13	0.2	2.5	0.3	0.43	$0.89*10^{-3}$	4.7	0,7	-	8
Limestone/aquifer	10	0.2	2.5	0.35	0.54	$0.89*10^{-3}$	4.7	0.7	4	8
Shale/Seal	5	0.2	2.3	0.01	0.01	$1.1*10^{-3}$	1.4	0.2	4	2
Sandstone	2.8	0.30	2	0.4	0.64	-	-	-	-	-

Possible values elastic properties for the used rock types

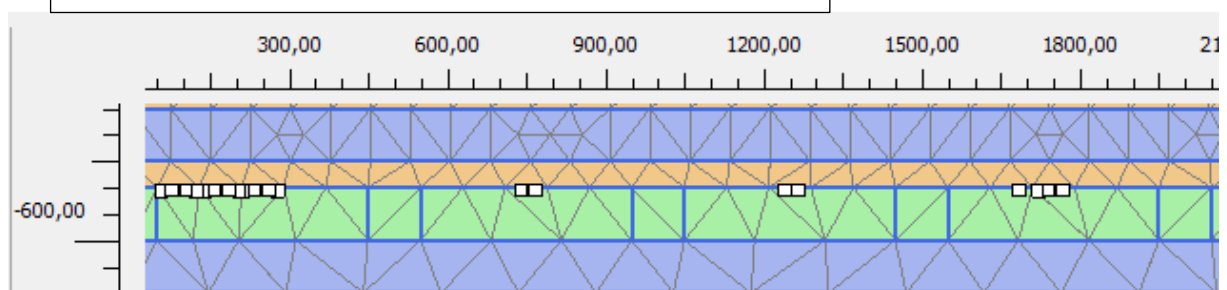
Rock type	Young's modulus (GPa)	Poisson's ratio
Sandstone	1-20	0.2-0.38
Shale	1-70	0.2-0.4
Limestone	15-55	0.18-0.33

Appendix E –

Picture of the slide from the lecture of Peter Schutjens



Creating fracture below the seal in Plaxis



In this figure, the tensile failure are shown as white dots. This indicates the occur of fracture and it happens below the seal and that is what we want to avoid.